Multi-omics profiling establishes the polypharmacology of FDA Approved CDK4/6 inhibitors and its impact on drug response

Marc Hafner*[,1,3], Caitlin E. Mills*[,1], Kartik Subramanian[1], Chen Chen[1], Mirra Chung[1], Sarah A. Boswell[1], Robert A. Everley[1], Changchang Liu[1], Charlotte S. Walmsley[2], Dejan Juric[1,2,ϕ], and Peter K. Sorger[1,†,ϕ]

* These authors contributed equally to this work.
ϕ These authors contributed equally to this work.

† Lead contact: Peter Sorger (peter_sorger@hms.harvard.edu, 617-432-6901/6902); orcid.org/0000-0002-3364-1838 copying Chris Bird (christopher_bird@hms.harvard.edu).

[1]Laboratory of Systems Pharmacology
Department of Systems Biology
Harvard Medical School
Boston, MA 02115

[2]Termeer Center for Targeted Therapies
Massachusetts General Hospital Cancer Center
Boston, MA 02114

[3]Current address:
Department of Bioinformatics & Computational Biology
Genentech, Inc.
South San Francisco, CA 94080

Running title: Advantageous polypharmacology of CDK4/6 inhibitors

ABSTRACT

The target profiles of many drugs are established early in their development and are not systematically revisited at the time of approval, raising the question whether human therapeutics with the same nominal targets but different chemical structures are functionally equivalent. In this paper we use five distinct phenotypic and biochemical assays to compare approved inhibitors of the cyclin-dependent kinases CDK4/6 (palbociclib, ribociclib, and abemaciclib) that are promising therapies for hormone-receptor positive breast cancer. We find that transcriptional, proteomic and phenotypic changes induced by the three drugs differ significantly and that abemaciclib has activates overlapping those of the older generation CDK inhibitor alvocidib. Abemaciclib's activities arise from inhibition of kinases other than CDK4/6 including CDK2/Cyclin A/E and CDK1/Cyclin B. Our data suggest the potential for differential use in the clinic and argue that a multi-faceted experimental and computational approach is necessary to obtain a reliable picture of kinase inhibitor target spectrum.

Key words: Therapeutics**,** targeted therapy; HR+ breast cancer; CDK4/6 inhibitors; drug profiling; drug mechanisms of action

INTRODUCTION

Progression through the cell cycle is controlled by over a dozen distinct protein complexes involving cyclins and cyclin-dependent kinases (CDKs). Because dysregulation of the cell cycle is a hallmark of cancer, several generations of CDK inhibitors have been tested as potential therapeutic agents. However, developing CDK inhibitors that are more active on tumor than normal cells has been a challenge and it is only recently that CDK4/6 inhibitors have emerged as promising therapies, particularly in breast cancer. CDK4 and CDK6 bind cyclin D early in the G1 phase of the cell cycle and phosphorylate the retinoblastoma protein (pRb). pRb is then hyper-phosphorylated by CDK2/cyclin E, relieving its inhibitory activities against transcription factors of the E2F family and allowing for S phase entry. Later in the cell cycle, CDK2/cyclin A and CDK1 in complex with cyclin A and B promote entry and progression through G2 and mitosis. Multiple genetic changes in cancer cells disrupt critical steps in cell cycle regulation: amplification of CDK4, CDK6, cyclin D, or cyclin E are common in solid tumors including breast cancers (Balko *et al.*, 2014; Asghar *et al.*, 2015). Deficiencies in pRb function, which cause unregulated S phase entry, as well as deletion of the CDK4/6 inhibitor p16 (encoded by *CDKN2A*) are also common (Franco, Witkiewicz and Knudsen, 2014; Asghar *et al.*, 2015).

First generation pan-CDK inhibitors active against cell cycle regulators such as CDK1/2/4/6 and transcriptional regulators such as CDK9 arrest cells in both G1 and G2 and were found to be broadly cytotoxic (Asghar *et al.*, 2015). Clinical development of these CDK inhibitors has been challenging largely because of poor therapeutic windows (Asghar *et al.*, 2015) thought to arise from a lack of selectivity for specific CDKs. Subsequent generations of CDK inhibitors were therefore designed to inhibit subsets of CDK proteins. In February 2015, the CDK4/6 inhibitor, palbociclib (PD0332991; Ibrance®) (Cristofanilli *et al.*, 2016) received FDA approval for management of hormone receptor-positive (HR^+) metastatic breast cancer (MBC) (Finn *et al.*, 2009; O'Leary, Finn and Turner, 2016). Subsequent clinical trials of the CDK4/6 inhibitors, ribociclib (LEE011; KISQALI®) (Hortobagyi *et al.*, 2016) and abemaciclib (LY2835219; Verzenio®) (Dickler *et al.*, 2016; Sledge *et al.*, 2017) also

demonstrated substantial improvements in progression-free survival in HR^+ metastatic breast cancer (Cristofanilli *et al.*, 2016; Griggs and Wolff, 2017) leading to their FDA approval. CDK4/6 inhibitors are currently regarded as some of the most promising new drugs for the treatment of HR^+ breast cancer and are also being tested against other malignancies (McCain, 2015; Goel *et al.*, 2016; Lim, Turner and Yap, 2016; Patnaik, Lee S. Rosen, *et al.*, 2016).

As observed with many other targeted therapies, however, acquired resistance to CDK4/6 inhibitors develops over time and nearly all initially responsive patients ultimately progress (Sherr, Beach and Shapiro, 2016). Resistance to CDK4/6 inhibitors is associated with multiple genomic alterations including amplification of Cyclin E, which promotes CDK2-dependent phosphorylation of pRb, amplification of CDK6, and loss of pRb function (Asghar *et al.*, 2015; Yang *et al.*, 2017). High expression of cyclin E is also associated with high CDK2 activity post-mitosis, which appears to bypass a requirement for CDK4/6 for cell cycle reentry (Asghar *et al.*, 2017).

Despite having the same nominal targets and similar initial clinical indications, emerging evidence suggests that palbociclib, ribociclib, and abemaciclib differ in the clinic: abemaciclib in particular has been reported to have single-agent activities and distinct adverse effects (Patnaik, Lee. S Rosen, *et al.*, 2016; O'Brien *et al.*, 2018). The three drugs are dosed differently, have different pharmacokinetics, and are reported to differ with respect to target selectivity (Kim *et al.*, 2013; Gelbert *et al.*, 2014; Chen, N. V. Lee, *et al.*, 2016; Cousins *et al.*, 2017). Among abemaciclib secondary targets examined to date, inhibition of DYRK/HIPK kinases is thought to contribute to cellular cytotoxicity (Knudsen *et al.*, 2017); inhibition of GSK3α/β can activate WNT signaling (Cousins *et al.*, 2017); but inhibition of CDK9 is thought to be therapeutically unimportant (Torres-guzmán *et al.*, 2017); Overall, however, the significance of differences in potency against CDK4/6 vs. other targets remains largely unexplored.

The target profiles of most clinical compounds are established relatively early in their development and are not necessarily revised at the time of approval. This is further complicated in the

case of kinase inhibitors by the use of different measurement technologies and the steady evolution of these technologies over the course of drug development. By directly comparing the target profiles and biological activities of palbociclib, ribociclib and abemaciclib, as well as an earlier generation pan-CDK inhibitor alvocidib (flavopiridol), we sought to address three questions: (i) are the three approved CDK4/6 inhibitors interchangeable with respect to biochemical and cell-based activities; (ii) is there a possibility that tumors that have become resistant to one CDK4/6 inhibitor might remain responsive to another inhibitor; and (iii) what are the relative merits of different approaches to characterizing the target spectrum of kinase inhibitors?

In this paper we report the analysis of CDK4/6 inhibitors using five experimental approaches that provide complementary insights into drug mechanisms of action: (i) mRNA sequencing of drug-perturbed cells, (ii) phosphoproteomics using mass spectrometry, (iii) GR-based dose-response measurement of cellular phenotypes (Hafner *et al.*, 2016), (iv) mRNA sequencing of drug-treated xenograft tumors and (v) three distinct types of *in vitro* analysis (activity assays with recombinant enzymes; kinome-wide profiling using the commercial KINOMEscan platform from DiscoverX (Fabian *et al.*, 2005); and kinase enrichment proteomics based on affinity purification on kinobeads (Duncan *et al.*, 2012). We find that the five experimental approaches provide different but complementary views of target coverage and demonstrate that palbociclib, ribociclib, and abemaciclib have differences in secondary targets and biological activities in breast cancer cell lines of varying genotypes. Multiple lines of evidence, including an *in vivo* xenograft model, show that the biological activities of abemaciclib arise from inhibition of kinases in addition to CDK4/6, notably CDK1/cyclin B and CDK2/cyclin E.

RESULTS

Approved CDK4/6 inhibitors induce distinct molecular signatures in breast cancer cells

To compare the mechanisms of action of palbociclib, ribociclib, and abemaciclib we performed transcriptional profiling (mRNA-seq) on a panel of seven breast cancer cell lines following 6 or 24 hours

of exposure to 0.3, 1 or 3 μM of drug (Figure 1a and Table S1). In all but pRb-deficient BT-549 cells, treatment with any of the three drugs gave rise to a signature (signature 1; Figure 1a in red) comprising 87 significantly down-regulated genes (FDR < 0.2). In addition, treatment of cells with abemaciclib in the low micromolar range induced a second transcriptional signature (signature 2; Figure 1a in cyan) that was absent from ribociclib-exposed cells and only weakly present in cells exposed to palbociclib. We queried the Broad Connectivity Map (CMAP) (Lamb *et al.*, 2006) with the two sets of down-regulated genes to determine which drug-induced changes they most closely matched. For signature 1, palbociclib and inhibitors of MEK (MAP kinase kinase) were the strongest hits (ribociclib and abemaciclib are absent from the CMAP dataset; Figure 1b and Table S2). Like CDK4/6 inhibition, MEK inhibition is anti-mitogenic in breast cancer cells, causing them to arrest at the G1/S transition (Meloche and Pouysségur, 2007; Caunt *et al.*, 2015). Gene set enrichment analysis showed that signature 1 was enriched for genes in the set *Reactome "Cell Cycle"* ($p=9.0\times10^{-50}$). Signature 1 therefore appears to reflect changes in gene expression associated with arrest in G1 (O'Leary, Finn and Turner, 2016). When signature 2 was compared to CMAP, the strongest hits were alvocidib and other pan-CDK inhibitors (Figure 1c and Table S2), suggesting that it arises from inhibition of CDKs other than CDK4 and CDK6. To determine the relative magnitude of the G1 arrest and pan-CDK inhibition phenotypes, we scored the absolute mean change in the expression of genes comprising signatures 1 and 2 for each condition. The G1-arrest score was high for all three drugs (Figure S1) whereas the strength of the pan-CDK score varied and was highest for abemaciclib above 0.3 μM and lowest for ribociclib; palbociclib treatment was associated with intermediate scores (Figure 1d).

To better understand the origins of the pan-CDK signature, we collected a substantially larger RNAseq dataset using the high throughput, low-cost RNA sequencing method 3' Digital Gene Expression (DGE-seq) (Soumillon *et al.*, 2014). Seven cell lines, including two that are pRB-deficient (BT-549 and PDX-1258), were exposed for 6 hours to palbociclib, ribociclib, or abemaciclib or to alvocidib (which inhibits CDK1/2/4/6/9); data were collected in triplicate at four CDK4/6 inhibitor

concentrations and two alvocidib concentrations. Differential expression of genes in signatures 1 and 2 (as defined above) was then used to compute G1-arrest and pan-CDK scores for each condition (Figure 2, Table S3). We found that the strength of the average pan-CDK scores was ordered as follows: alvocidib > abemaciclib > palbociclib > ribociclib (Figure 2, x-axis). The pan-CDK signature was also strongly dose-dependent for abemaciclib ($r=0.78$, $p=9.3\times10^{-7}$) and alvocidib ($r=0.76$, $p=1.5\times10^{-3}$). Notably, the score for 0.1 μM and 1 μM alvocidib across all cell lines (green) substantially overlapped abemaciclib at 1 μM and 3 μM (red). G1 arrest scores were dose-dependent for all drugs and substantially higher in pRB-competent than in pRb-deficient cell lines (0.73 vs. 0.25). In the case of ribociclib, only four genes belonging to the G1 signature were differentially regulated in pRB-deficient lines (two-sided Fisher exact test $p=2\times10^{-4}$ as compared to pRB-proficient lines) consistent with the hypothesis that a pure CDK4/6 inhibitor should be inactive in cells lacking pRB, the primary substrate of CDK4/6 kinases. In the case of alvocidib, abemaciclib and palbociclib a non-zero G1 signature most likely arises in pRB-deficient cells because pan-CDK and G1 arrest signatures are not orthogonal and the inhibition of CDKs other than CDK4/6 makes a contribution. However, the converse is not true: a high G1-arrest score can be associated with a pan-CDK score near zero. Taken together, the transcript profiling data strongly suggest that palbociclib, ribociclib, and abemaciclib have different target spectra in breast cancer cells with abemaciclib, and to a lesser extent palbociclib, having features in common with alvocidib. Like alvocidib, abemaciclib is biologically active in pRB-deficient cells, which also demonstrates CDK4/6-independent activities.

Effects of CDK4/6 inhibitors on the activity of CDK/cyclin complexes

To study the effects of CDK4/6 inhibitors on the phosphoproteome we performed isobaric (TMT) tag based liquid-chromatography mass spectrometry (LC/MS) (McAlister *et al.*, 2012). MCF7 cells were treated with DMSO, palbociclib, or abemaciclib for one hour (to focus on immediate-early changes in the phosphoproteome) and a total of 9958 phosphopeptides were detected across all samples;

among these 739 were down-regulated in the presence of palbociclib and 2287 in the presence of abemaciclib (log2 fold-change > 1.5; Figure 3a, Table S4). Enrichment analysis (Drake *et al.*, 2012) involving known kinase-substrate relationships (see Methods) was used to identify kinases whose down-regulation was most likely to account for observed phosphoproteome changes. This analysis showed that inferred activities for CDK4, CDK6, and Aurora A/B kinases (AURKA/B) were significantly down-regulated in both palbociclib and abemaciclib-treated cells and CDK1, CDK2, CaM-kinase II subunit alpha (CAMK2α), TTK, and polo-like kinase 1 (PLK1) were downregulated only in the presence of abemaciclib (Figure 3b, Table S5). Thus, phosphoproteome profiling confirms that abemaciclib has a greater effect on the activity of the kinome than palbociclib and that inhibition of CDKs other than CDK4 and CDK6 is likely involved.

Inference of kinase activity from phosphoproteome data yields both direct and indirect drug targets. We therefore performed three different *in vitro* assays to identify direct targets. KINOMEscan, available as a service from DiscoverX, involves an affinity binding assay between members of a 468 DNA-tagged recombinant kinase library and an immobilized ATP-like ligand; the assay is performed in the presence and absence of an ATP-competitive drug (Fabian *et al.*, 2005). KINOMEscan profiling showed that ribociclib is the most selective CDK4/6 inhibitor and abemaciclib the least (Figure 3c, Figure S2a-b and Table S6); similar data are found in (Gelbert *et al.*, 2014; Chen, N. V Lee, *et al.*, 2016).

Since several CDKs are not found in the KINOMEscan library (e.g. CDK1, CDK6) or are not complexed with cyclins (e.g. CDK2), we also used multiplexed inhibitor bead mass spectrometry (MIB/MS) (Duncan *et al.*, 2012) to obtain kinome profiles. In this assay, a cell lysate is mixed with beads conjugated to pan-kinase inhibitors in the presence and absence of a test drug and the levels of bound kinases then determined by mass spectrometry (Figure 3d, Table S7); to generate a lysate with the greatest number of expressed kinases we mixed several cell types (Médard *et al.*, 2015). We detected 164 kinases, including 13 CDKs in the unfractionated extract by TMT LC/MS, and found that ribociclib,

palbociclib, and abemaciclib all bound to CDK4 and CDK6. In addition, abemaciclib bound to CDK1, CDK2, CDK7 and CDK9; for abemaciclib we also observed strong binding to GSK3α/β and CAMK2γ/δ. These results agreed well with data for abemaciclib recently published by Cousins et al (Spearman's $\rho = 0.62$, $P = 8.9\times10^{-16}$) (Cousins *et al.*, 2017). Moreover, when KINOMEscan data (obtained in the presence of 1 μM abemaciclib) and MIB data (obtained with 10 μM abemaciclib) were compared, 19 of 25 kinases strongly inhibited in the KINOMEscan and also found in cell extracts were significantly reduced in binding to MIBs (log2 fold change > 1.5), demonstrating good reproducibility between different types of assays. We conclude that ribociclib is the most selective CDK4/6 inhibitor tested and abemaciclib the least, with a dose-dependent increase in the number of targets significantly inhibited by abemaciclib from 4 at 0.1 μM drug to 13 at 1 μM and 28 at 10 μM.

To quantify drug effects on individual kinases, we performed in vitro activity assays (SelectScreen assays by Thermo Fisher or HotSpot assays by Reaction Biology; see Methods) at 10 drug concentrations using recombinant human kinases and kinase-cyclin complexes identified as potential targets by transcriptional, phospho-proteomic or kinase profiling assays. The data showed that abemaciclib was the most potent inhibitor of CDK4 and CDK6 and confirmed activity against multiple kinases that were not inhibited, or were only weakly inhibited, by palbociclib or ribociclib (Figure 3e, Figure S3a and Table S8). These kinases include CDK2/cyclin A/E, CDK1/cyclin B, CDK7/cyclin H, CDK9/cyclin K/T1, GSK-3β, CAMK2A, and TTK (Figure S3b). In comparison to the first-generation CDK inhibitor alvocidib, abemaciclib is similar in its activity against CDK2/cyclin A/E and about 10-fold less active against CDK1/cyclin B, CDK7/cyclin H, and CDK9/cyclin K/T1 (potentially explaining the improved toxicity profile of abemaciclib relative to pan-CDK inhibitors), whereas ribociclib and palbociclib were at least one order of magnitude less potent against these kinases. The potency of the three drugs against CDK4 vs. CDK6 was dependent on the cyclin partner and the assay, but the kinases generally differed by no more than 3-fold (Table S8). Results from KINOMEscan, kinobead, and SelectScreen assays were generally concordant with mRNA-seq and phosphoproteome profiling with

three notable exceptions: CDK1 and CDK6 are absent from the KINOMEscan panel and CDK2, while present, does not appear to be active, perhaps because CDK2/cyclin complexes do not form (Echalier *et al.*, 2014). Thus, the widely used KINOMEscan assay misses the ability of abemaciclib to inhibit CDK2-cyclin A/E complexes, an activity that is potentially significant given the ability of these complexes to rescue CDK4/6 inhibition.

Comparing CDK4/6 inhibitors in breast cancer cell lines

To compare the biological activities of CDK4/6 inhibitors, we acquired dose-response curves in 34 breast cancer cell lines spanning all clinical subtypes and computed GR values (Figure 4a and Table S9), which distinguish between drug-induced cell cycle arrest and cell death while correcting for apparent differences in drug sensitivity arising from variable proliferation rates (Hafner *et al.*, 2016; Hafner, Niepel and Sorger, 2017). Both palbociclib and abemaciclib elicited cytostatic responses with GR_{50} values in the 10-100 nM range (Table S10). Potency was highly correlated among the drugs (Spearman's $\rho = 0.91$, $P = 5.7\times10^{-14}$) with abemaciclib ~5.5-fold more potent on average in inducing cytostasis (t-test $P = 5.3\times10^{-7}$); this difference is consistent with a 3-fold difference between palbociclib and abemaciclib in *in vitro* IC_{50} values for CDK4/6 inhibition (as measured *in vitro* by SelectScreen assays; Figure 3e). Efficacy measured by GR values at 0.1 μM varied between 0 (complete cytostasis) and 0.76 (weak growth inhibition) depending on the cell line and was similar for palbociclib and abemaciclib, showing that at these concentrations the drugs only fractionally inhibit cell proliferation. In pRb-deficient cell lines, palbociclib was inactive and abemaciclib had little or no effect below 0.3 μM (yellow lines Figure 4a); thus, the cytostatic response is likely to be a result of CDK4/6 inhibition.

However, abemaciclib also elicited a second response at doses greater than 0.3 μM; this response was characterized by negative GR values and cell death (see Methods; Figure 4a). As a result, the complete dose-response behavior of abemaciclib was significantly better fitted in most cell lines by the product of two sigmoidal curves (Figure 4b, Figure S4, and Methods). The mid-point of the second

response curve was offset to a similar degree as *in vitro* dose-response curves for CDK1/2 vs. CDK4/6 inhibition (Table S8). This behavior is consistent with inhibition of two sets of targets: CDK4/6 at low dose – resulting in G1 arrest – and kinases such as CDK1/2 above 0.3 μM – resulting in cell death. The high-dose drop in GR values was not observed in palbociclib-treated cells nor in the eight cell lines in which GR data were collected for ribociclib. As a result, abemaciclib was substantially more efficacious than palbociclib in inhibiting and killing pRb-proficient cells of all subtypes, having a GR_{max} value on average 0.52 below that of palbociclib (t-test P=4.5×10^{-9}; Table S10).

When we searched a set of 30 cell cycle regulators for those whose mRNA expression levels could discriminate between responsiveness to palbociclib and abemaciclib in pRb-proficient cell lines, and potentially explain variability in abemaciclib-mediated cytotoxicity, we found that a combination of elevated expression of CDKN1A (p21 – an inhibitor of CDK1/2/4/6), CDKL5 (a cyclin-dependent kinase targeted by abemaciclib and other pan-CDK inhibitors based on KINOMEscan data), CCNE1 (cyclin E1, which has been implicated in palbociclib resistance (Sherr, Beach and Shapiro, 2016)) and reduced expression of CDK9 (another abemaciclib and pan-CDK inhibitor target) comprised a strong preclinical pharmacogenomic predictor across the 26 cell lines tested (q^2 = 0.85, P = 2.9×10^{-6} by leave-one-out cross validation; Figure 4c-d).

Abemaciclib blocks cells in the G2 phase of the cell cycle

Consistent with the known biology of CDK4/6 inhibition, abemaciclib, ribociclib, and palbociclib all suppressed pRb phosphorylation and arrested cells in G1 (Figure 5a). The 3-fold difference in drug concentration needed to induce arrest matched measured differences in potency in biochemical assays (with abemaciclib the most potent and ribociclib the least; Figure 3e). A fraction of cells treated with abemaciclib also arrested in G2 rather than G1, particularly at drug concentrations of 0.3 μM and above (Figure 5a, Figure S5a), a possible consequence of inhibition of CDK1 and CDK2, whose activities are required for progression through mitosis and S-phase. Treating pRb-deficient cells

with ribociclib or palbociclib had no effect on proliferation whereas treatment with abemaciclib caused cells to accumulate in G2, consistent with an abemaciclib-induced cell cycle arrest independent of CDK4/6 (Fig. 5b, Fig. S5a-b).

When we compare the scores for G1-arrest and pan-CDK signatures across a range of doses in multiple cell lines we found that pan-CDK score was significant for abemaciclib only above 0.3 μM (P=2.1×10^{-4}, ranksum test); activity was observed in pRB-deficient cells only at concentrations of 1 μM and above. When a drug inhibits multiple targets with different potencies, as observed for abemaciclib, the question arises whether both primary and secondary targets can be engaged at doses achievable *in vivo*. The maximum serum concentration in humans (C_{max}) for abemaciclib is estimated to be 0.5 μM to 1 μM when active metabolites are included (Burke *et al.*, 2016; Patnaik, Lee S. Rosen, *et al.*, 2016) suggesting abemaciclib could have activities such as induction of cell death and G2 arrest at concentrations relevant to clinical use.

Assaying abemaciclib polypharmacology in xenograft tumors

To directly test the hypothesis that abemaciclib is active against kinases other than CDK4/6 in vivo, we generated MCF-7 xenografts in nude mice and exposed them to CDK4/6 inhibitors at a range of doses. When tumors reached ~300 mm^3, animals were randomly assigned to treatment groups and treated daily for 4 days to a vehicle-only control or to 150 mg/kg ribociclib, 150 mg/kg palbociclib or 25-150 mg/kg abemaciclib, doses previously shown to be effective in xenografts (Fry *et al.*, 2004; Gelbert *et al.*, 2014; O'Brien *et al.*, 2014). Animals were euthanized and tumors divided into two samples; one was fixed in formaldehyde and paraffin embedded and the other processed for mRNA-sequencing. FFPE specimens were imaged by immunofluorescence using vimentin and E-cadherin staining to distinguish tumor cells from mouse stroma. We found that all conditions tested resulted in a significant reduction in the fraction of p-pRb positive cells (Dunnett's multiple comparison $P < 0.0001$) providing pharmacodynamic evidence that all tumors were exposed to drug at active concentrations

(Figure 6a). mRNA-seq data showed that all three drugs induced a G1-arrest signature (Figure 6b, Table S11), the strength of which was correlated with the degree of p-pRb inhibition (Spearman's $\rho = -0.80$, $P = 1.1\times10^{-10}$). Furthermore, at doses above 100 mg/kg, abemaciclib (but not ribociclib or palbociclib) also induced a strong pan-CDK signature (Figure 6b). These data provide *in vivo* confirmation that abemaciclib can engage targets other than CDK4 and CDK6, recapitulating the drug's off-target activity in cell culture.

Abemaciclib prevents adaptive response in contrast to palbociclib and ribociclib

As previously described (Herrera-Abreu *et al.*, 2016; Asghar *et al.*, 2017), cells adapt to CDK4/6 inhibition over time. Within 48 hours of exposure to palbociclib or ribociclib we found that cells re-entered the cell cycle and acquired a p-pRb positive state at drug concentrations as high as 3.16 μM (Figure 5a). In contrast, pRb phosphorylation remained low in cells exposed to 1 μM abemaciclib and above (Figure 5a) with ongoing cell death and no evidence of adaptation five days after drug exposure (Figure 7a, Figure S6 and Table S12). In studies designed to assess long-term adaptation to drug, we observed that breast cancer cells grown for several months in the presence of 1 μM palbociclib had higher cyclin E (CCNE1) and lower pRb levels than parental cells (Figure 7b). These palbociclib-adapted cells were cross-resistant to ribociclib (Figure 7c, Figure S7a-b and Table S13) but sensitive to abemaciclib at doses of 1 μM and above, consistent with the ability of abemaciclib to target kinases not inhibited by palbociclib.

We also established a cell line from a patient with advanced/metastatic $HR^+/Her2^-$ breast cancer whose disease had progressed following eight months on ribociclib/letrozole. The tumor lacked pRb by immunohistochemistry (Figure 7c) as did the derived cell line (MGH312; Figure S7d). These tumor cells were responsive to abemaciclib as judged by inhibition of cell proliferation and induction of cell death but were completely resistant to palbociclib or ribociclib even at high doses (Figure 7d and Table S14). It will remain unknown, however, whether or not this patient (now deceased) could have benefited

from treatment with abemaciclib. Nonetheless, we propose that abemaciclib may have clinically useful activities in a subset of tumors that are not responsive, or have become resistant to, more selective CDK4/6 inhibitors.

DISCUSSION

It is not uncommon for multiple therapeutics targeting the same proteins to be approved in close succession. In the case of CDK4/6 inhibitors, palbociclib, ribociclib and abemaciclib have all proven to be highly effective in the treatment of HR^+ metastatic breast cancer and are currently being tested in ~100 ongoing clinical trials for activity in other malignancies. It has hitherto been assumed that the mechanisms of action of the three approved drugs are very similar, and distinct from those of older-generation CDK inhibitors such as alvocidib: observed differences in the efficacy and toxicity of palbociclib, ribociclib and abemaciclib have been attributed to differences in dosing schedules or potency against CDK4 versus CDK6 (Sherr, Beach and Shapiro, 2016). However, the current paper presents six lines of evidence that ribociclib, palbociclib, abemaciclib and alvocidib actually span a spectrum of selectivity for CDK-cyclin complexes. In particular, Abemaciclib has biochemical and physiological activities not manifest by ribociclib and only weakly by palbociclib. First, exposure of breast cancer cells of different subtypes to CDK4/6 inhibitors induces transcriptional changes associated with G1 arrest and in the case of abemaciclib alone, to dose-dependent transcriptional changes similar to those elicited by alvocidib and arising from pan-CDK inhibition. Second, exposing cells to abemaciclib results in more extensive changes in the phosphoproteome than exposure to palbociclib and kinase inference suggests that this is due in part to inhibition of CDK1 and CDK2. Third, kinome profiling using industry-standard KINOMEscan panels, multiplexed inhibitor bead mass spectrometry, and kinase activity assays confirms that abemaciclib has multiple targets in addition to CDK4/6. Fourth, abemaciclib causes arrest of cells in both the G1 and G2 phases of the cell cycle and the drug is cytotoxic even in the absence of pRb; in contrast, cells exposed to palbociclib and ribociclib arrest only

in G1 and elicit little or no cell death. Fifth, in a mouse xenograft model, abemaciclib induces both CDK4/6-like G1 arrest and pan-CDK transcriptional signatures, as observed in cultured cells. Sixth, whereas abemaciclib durably inhibits cell division, cultured cells adapt within 2-3 days of continuous exposure to palbociclib or ribociclib and resume proliferation. Moreover, a cell line derived from a patient with $HR^{+}/Her2^{-}$ breast cancer that progressed on ribociclib/letrozole remained sensitive to abemaciclib.

Evidence of substantial differences among CDK4/6 inhibitors is scattered throughout the literature but has not been consolidated or rigorously evaluated, consistent with a general lack of comparative biochemical data on many FDA-approved drugs. Large-scale kinase profiling studies using KINOMEscan or MIB/MS are one exception to this generalization (Fabian *et al.*, 2005; Gelbert *et al.*, 2014; Cousins *et al.*, 2017; Klaeger *et al.*, 2017). However, our findings strongly argue for a multi-faceted approach to comparative mechanism of action studies. Proteomic, transcriptional, biochemical, and phenotypic assays measure different aspects of drug action and in the current work a combination of methods was needed to obtain a complete picture of target spectrum. For example, the false negative finding in KINOMEscan data that abemaciclib does not interact with CDK2 may explain why biological differences among CDK4/6 inhibitors have not been widely appreciated. Similarly, whereas GSK3β was found to be an abemaciclib target of borderline significance by phospho-proteome profiling, perhaps reflecting the challenges of inferring changes in kinase activity from data that are inherently under-sampled (Riley and Coon, 2016), it was clearly a target by kinase activity assays (Cousins *et al.*, 2017). Conversely, mRNA and proteomic profiling assays showed that exposure of breast cancer cells to abemaciclib results in inhibition of CDK9, AURKA/B, CAMK2α, TTK, and PLK1 but biochemical experiments showed that AURKA/B and PLK1 are most likely indirect targets of abemaciclib whose activity is downregulated as a secondary consequence of G2 cell cycle arrest (the other kinases appear to be direct targets of abemaciclib). Consistent with Cousins et al. (Cousins *et al.*, 2017), our results using multiple different assays provide little support for the assertion that ribociclib, palbociclib or

abemaciclib are systematically more active against CDK4 than CDK6. Instead, the opposite appears to be true: enzymatic assays show the IC_{50} for CDK4 is about 2.5-fold greater than for CDK6 for all three drugs. Thus, despite frequent assertions that difference in the CDK4/6 ratio among the three drugs might therapeutically significant (Gelbert *et al.*, 2014; Patnaik, Lee S. Rosen, *et al.*, 2016; Patnaik, Lee. S Rosen, *et al.*, 2016) our data suggest that this is unlikely as both targets are likely to be highly inhibited at therapeutic doses.

In the case of a poly-selective drug such as abemaciclib the question arises whether activities observed at different drug concentrations are all biologically relevant. There is no question that CDK4 and CDK6 are the highest affinity targets of abemaciclib and that abemaciclib is the most potent of the three approved drugs against these CDKs. Abemaciclib is 10- to 100-fold less potent against CDK2 and CDK1 than CDK4/6, but we detect the cellular consequences of CDK1/2 inhibition in cell lines at concentrations as low as 0.3 μM, well within the C_{max} range in humans, and also achievable in xenograft mouse models (Raub *et al.*, 2015; Burke *et al.*, 2016; Patnaik, Lee S. Rosen, *et al.*, 2016). Abemaciclib also exhibits substantially reduced drug adaptation with respect to anti-proliferative effects, which is beneficial for an anti-cancer drug.

The current generation of CDK4/6 inhibitors has benefited from a considerable investment in increasing target selectivity, mainly as a means of reducing toxicity relative to earlier generation drugs (Toogood *et al.*, 2005; Asghar *et al.*, 2015; Peplow, 2017). However, our findings suggest that abemaciclib is not equivalent to palbociclib or ribociclib. Its activities against kinases other than CDK4/6 are beneficial for anti-cancer activity and targeting them jointly with CDK4/6 may be a means to achieve more durable responses than with CDK4/6 inhibition alone. Inhibition of CDK1/7/9 may also contribute to cell killing (Kitada *et al.*, 2000; Wittmann *et al.*, 2003) and inhibition of mitotic kinases such as TTK may enhance tumor immunogenicity, a key contributor to drug response (Luen *et al.*, 2016). Blocking CDK2/cyclin E should mitigate resistance resulting from amplification of cyclin E

(Dean *et al.*, 2010; Herrera-Abreu *et al.*, 2016) and also achieve a more complete therapeutic response by targeting mitotic cells with high CDK2 activity (Asghar *et al.*, 2017).

These findings provide a rationale for treating patients with abemaciclib following disease progression on palbociclib or ribociclib: cells, including cells derived from a patient, that have become resistant to these two drugs remain sensitive to abemaciclib. The enhanced activities of abemaciclib relative to other CDK4/6 inhibitors are observed at concentrations of 0.3 μM and above, overlapping human C_{max} concentrations. However, further studies are needed to determine how *in vitro* efficacy translates to patients and if incremental benefit from treatment with abemaciclib is observed. This is particularly true in the case of pRb-deficient tumors, in which abemaciclib's efficacy relies on micromolar concentrations. An alternative is to combine CDK4/6 inhibitors with drugs that inhibit abemaciclib's secondary targets or develop molecules that jointly inhibit CDK4/6 and CDK2, a strategy Pfizer is pursuing (US patent 20180044344A1). In all of these cases, our work shows that polypharmacology can be exploited to achieve more durable responses than with "pure" CDK4/6 inhibitors such as ribociclib.

SIGNIFICANCE

The target profiles of most drugs are established relatively early in their development and are not systematically revisited at the time of approval. Scattered reports suggest that palbociclib, ribociclib, and abemaciclib differ in pharmacokinetics, dosing, and adverse effects but the three drugs are generally regarded as similar. Our finding that the drugs differ substantially in mechanism of action – abemaciclib retains activities of the earlier-generation drug alvocidib – suggests the potential for different uses in the clinic: in particular, abemaciclib may show activity in patients progressing on palbociclib or ribociclib. More generally, our approach relying on data from five distinct phenotypic and biochemical assays strongly suggests that a multi-faceted approach is necessary to get a reliable picture of the target spectrum of kinase inhibitors.

Acknowledgements. This work was funded by P50-GM107618, U54-CA225088 and U54-HL127365 to PKS and DJ. We thank LSP member M. Berberich for skilled assistance, the ICCB for help with automation, S. Gygi for use of software and computing facilities for proteomics, and A. Bardia for comments.

Author contributions. MH, CEM, and DJ conceived the study; MH, CEM, DJ, and PKS designed the experiments and CEM, MC, SAB, and RAE performed them. MH, KS, and CC performed the computational analyses. CSW and DJ obtained the patient-derived line and provided related data. PKS oversaw the experimental and computational research; MH, CEM, KS, DJ, and PKS wrote the manuscript.

Declaration of interest. M. Hafner is currently an employee of Genentech, Inc and declares no conflicts of interest. R. Everley is currently an employee of Pfizer, Inc and declares no conflicts of interest. Dr. Juric reports personal fees from Novartis, Genentech, Eisai, Ipsen, and EMD Serono, during the conduct of the study. Other authors have no conflict of interest.

FIGURE LEGENDS

Figure 1: Transcriptional responses of breast cancer cell lines to CDK4/6 inhibitors. (a) Clustering of transcriptional response for seven breast cancer cell lines treated for 6 or 24 hours with ribociclib, palbociclib, or abemaciclib at 0.3, 1, or 3 μM. Only genes for which statistically significant (FDR < 0.2) changes were observed in at least 3 conditions are shown. Down-regulated genes comprising signature 1 and 2 are outlined in red and cyan, respectively. **(b-c)** Enrichment scores for signature 1 (b) and 2 (c) based on L1000 signatures identified by Enrichr (see Methods). **(d)** Score of the pan-CDK transcriptional signature per cell line following six hours of exposure to drug based on the RNA-seq data from panel (a).

Figure 2: G1-arrest and pan-CDK scores induced by CDK4/6 inhibitors. Score of the G1-arrest signature relative to the pan-CDK signature for seven cell lines treated with palbociclib, ribociclib, abemaciclib or alvociclib at 0.1, 0.3, 1, or 3 μM; squares denote pRb-deficient lines. Distributions of scores for pRb-competent lines are shown at the margins for each signature.

Figure 3: inhibition of CDK/cyclin activity by CDK4/6 inhibitors. (a) Clustering of changes in phosphopeptide levels for MCF7 cells treated for 1 hour with either abemaciclib or palbociclib at 0.3 or 3 μM. **(b)** Normalized enrichment scores for kinases based on the phosphoproteomic data in panel (a). Only kinases inferred as down-regulated in at least two conditions are displayed; drugs and concentrations at which differences are significant (FDR < 0.2) are shaded. **(c)** Inhibition of the top 100 inhibited kinases plus CDK2, and AURKA at 0.1 and 1 μM of each CDK4/6 inhibitor measured by the KINOMEscan assay (see Figure S2). **(d)** The degree of inhibition (log2 fold change) of each CDK detected by MIB/MS after treating a mixed cell lysate with a CDK4/6 inhibitor at the doses indicated. **(e)** *In vitro* kinase activity assays confirm inhibition of additional targets by abemaciclib. Comparison of

IC$_{50}$ values for CDK4/6 inhibitors and alvocidib as measured using purified kinases and 10-point *in vitro* dose-response assays (see Figure S3).

Figure 4: Comparison of the phenotypic response of breast cancer cell lines to CDK4/6 inhibitors. **(a)** GR curves for cell growth (top) and increased percent of dead cells over vehicle-only control conditions (bottom) for 26 pRb-proficient breast cancer cell lines (blue) and 8 pRb-deficient cell lines (yellow) treated with palbociclib (left) or abemaciclib (right) for 72 hours. The vertical box illustrates the maximum serum concentration for abemaciclib (C_{max}). **(b)** Dose-response curve for palbociclib (red) and abemaciclib (blue) in MCF7 cells. Dotted lines depict two fitted sigmoidal curves whose product optimally recapitulates the blue curve with extracted values for GEC_{50} (50%-maximal effective concentration) shown below and for GR_{max} (maximal efficacy) shown to the right (See Figure S4). **(c)** Performance of a pharmacogenomics predictor of palbociclib vs. abemaciclib drug response based on mRNA levels for 30 cell cycle regulators; plots shows the observed versus predicted (leave-one-out cross validation) difference in GR value at 3 μM between palbociclib and abemaciclib based on a linear model of **(d)** The predictor coefficients from the model in (c), error bars represent the standard error of the model.

Figure 5: Comparison of the effects of ribociclib, palbociclib, and abemaciclib on the cell cycle. (a) Distribution of DNA content in MCF7 cells exposed to one of three CDK4/6 inhibitors over a range of concentrations for 24 (left) or 48 (right) hours. In each curve the phospho-pRb positive cell population is depicted in a darker shade. One representative replicate out of three is shown. **(b)** Distribution of DNA content for PDX12-58 cells, which are pRb-deficient, exposed to abemaciclib for 48 hours at a range of concentrations (see Figure S6 for palbociclib and ribociclib results). These data represent one of three biological replicates.

Figure 6: Transcriptional response of MCF-7 xenografted cells to CDK4/6 inhibitors

(a) Fraction of phospho-pRb positive tumor cells in MCF-7 xenografts after four days of drug treatment. **(b)** Score of the pan-CDK transcriptional signature as compared to the G1-arrest signature across MCF-7 tumors following four days of exposure to drug; same analysis as in Figure 2.

Figure 7: Acute and adaptive responses of breast cancer cell lines and tumors to CDK4/6 inhibitors. (a) Time-dependent GR values for MCF7, Hs 578T, and PDX12-58 cells treated with 3.16 μM ribociclib, palbociclib, or abemaciclib for five days (increased percent of dead cells over vehicle-only control conditions shown in Figure S6). One representative replicate out of four is shown. **(b)** Western Blots of cyclin E and total pRb levels in Hs 578T and MCF7 parental cells and cells adapted to grow in 1 μM palbociclib. **(c)** GR values for Hs 578T and MCF7 parental cells and cells adapted to grow in 1 μM palbociclib in response to treatment with 3.16 μM ribociclib, palbociclib, or abemaciclib for 72 h (see Figure S7). * denotes $P < 0.05$; ** denotes $P < 0.01$ as measured using a t-test with six replicates in each group. Error bars denote SEM of six replicates. **(d)** GR values (left) and increased percent of dead cells over vehicle-only control conditions (right) for the patient-derived line MGH312 in response to 96-hour treatments with ribociclib, palbociclib, or abemaciclib. Error bars show the SEM of three replicates.

SUPPLEMENTAL FIGURE LEGENDS

Figure S1, Related to Figure 1: G1-arrest transcriptional signature score. Score of the G1-arrest transcriptional signature per cell line following 6 hours of exposure to drug based on the RNA-seq data from Fig 1a.

Figure S2, Related to Figure 3: KINOMEscan results for the three CDK4/6 inhibitors. (a) Kinases with less than 10% activity remaining for drug concentrations of 0.1 μM and 1.0 μM of each of the three CDK4/6 inhibitors (see Table S6). Images generated using the TREEspotTM Software Tool and reprinted with permission from KINOMEscan®, a division of DiscoveRx Corporation, © DISCOVERX CORPORATION 2010. **(b)** The differential binding between 0.1 μM and 1.0 μM of the 100 most bound kinases, plus CDK2 and AURKA, for all drugs.

Figure S3, Related to Figure 3: In vitro activity of CDK4/6 inhibitors and alvocidib. (a) Unbound fraction or inhibition curves for select kinase targets with increasing concentrations of CDK4/6 inhibitors or alvocidib (see Methods for assay details). Error bars are the SEM of two replicates. **(b)** Comparison of IC_{50} values for CDK4/6 inhibitors and alvocidib for select kinases and CDK/cyclin complexes.

Figure S4, Related to Figure 4: Comparison of fit parameters defined in Fig. 4b for the dose response curves for palbociclib and abemaciclib shown in Fig. 4a. (top) Mid-point concentrations for palbociclib (left) and the 2nd phase of abemaciclib (right) versus the mid-point concentrations for the 1st phase of abemaciclib. (bottom) Maximal efficacy for 1st phase of abemaciclib (left) and abemaciclib (right) versus the maximal efficacy of palbociclib.

Figure S5, Related to Figure 5: Effect of CDK4/6 inhibitors on the distribution of cells through the cell cycle. (a) DNA content versus EdU intensity for three breast cancer cell lines either untreated or

treated for 24 hours with 1.0 μM of ribociclib, palbociclib, or abemacicib (from left to right). Color intensity reflects density of cells; numbers represent the percentage of cells in each phase of the cell cycle based on automated gating (blue lines). **(b)** Distribution of DNA content for PDX12-58 cells, which are pRb-deficient, exposed to either ribociclib or palbociclib for 48 hours at a range of concentrations. These data represent one of three biological replicates.

Figure S6, Related to Figure 7: Time dependent increase in the fraction of dead cells treated with CDK4/6 inhibitors. Increased percent of dead cells treated with 3.16 μM ribociclib, palbociclib, or abemaciclib relative to control conditions over time (see Fig. 7a).

Figure S7, Related to Figure 7: Characterization of CDK4/6-inhibitor resistant cell lines. (a) GR values for cell lines adapted to grow in 1 μM palbociclib and their parental lines in response to 72-hour treatments with ribociclib, palbociclib, or abemaciclib. Error bars show the SEM of six replicates. **(b)** Increased percent of dead cells over vehicle-only control conditions for cell lines adapted to grow in 1 μM palbociclib and their parental lines in response to 72-hour treatments with ribociclib, palbociclib, or abemaciclib. Error bars show the SEM of six replicates. **(c)** pRb immunohistochemistry staining of the patient biopsy at the site from which the cell line MGH312 was derived. **(d)** Western Blot of pRb for MCF7, BT-549, and MGH312 cells.

REFERENCES

Asghar, U. *et al.* (2015) 'The history and future of targeting cyclin-dependent kinases in cancer therapy', *Nature Reviews Drug Discovery*. Nature Publishing Group, 14(2), pp. 130–146. doi: 10.1038/nrd4504.

Asghar, U. *et al.* (2017) 'Single-Cell Dynamics Determines Response to CDK4/6 Inhibition in Triple-Negative Breast Cancer.', *Clinical cancer research : an official journal of the American Association for Cancer Research*, 23(18), pp. 5561–5572. doi: 10.1158/1078-0432.CCR-17-0369.

Balko, J. M. *et al.* (2014) 'Molecular profiling of the residual disease of triple-negative breast cancers after neoadjuvant chemotherapy identifies actionable therapeutic targets.', *Cancer discovery*, 4(2), pp. 232–45. doi: 10.1158/2159-8290.CD-13-0286.

Beausoleil, S. A. *et al.* (2006) 'A probability-based approach for high-throughput protein phosphorylation analysis and site localization.', *Nature biotechnology*, 24(10), pp. 1285–92. doi: 10.1038/nbt1240.

Burke, T. *et al.* (2016) 'Abstract 2830: The major human metabolites of abemaciclib are inhibitors of CDK4 and CDK6', *Cancer Research*, 76(14 Supplement), pp. 2830–2830. doi: 10.1158/1538-7445.AM2016-2830.

Caunt, C. J. *et al.* (2015) 'MEK1 and MEK2 inhibitors and cancer therapy: the long and winding road.', *Nature reviews. Cancer*, 15(10), pp. 577–92. doi: 10.1038/nrc4000.

Chen, P., Lee, N. V, *et al.* (2016) 'Spectrum and Degree of CDK Drug Interactions Predicts Clinical Performance', (i), pp. 1–11. doi: 10.1158/1535-7163.MCT-16-0300.

Chen, P., Lee, N. V., *et al.* (2016) 'Spectrum and Degree of CDK Drug Interactions Predicts Clinical Performance.', *Molecular cancer therapeutics*, 15(10), pp. 2273–2281. doi: 10.1158/1535-7163.MCT-16-0300.

Cousins, E. M. *et al.* (2017) 'Competitive Kinase Enrichment Proteomics Reveals that Abemaciclib Inhibits GSK3β and Activates WNT Signaling', *Molecular Cancer Research*. Available at: http://mcr.aacrjournals.org/content/early/2018/01/10/1541-7786.MCR-17-0468.abstract.

Cristofanilli, M. *et al.* (2016) 'Fulvestrant plus palbociclib versus fulvestrant plus placebo for treatment of hormone-receptor-positive, HER2-negative metastatic breast cancer that progressed on previous endocrine therapy (PALOMA-3): final analysis of the multicentre, double-blind, phas', *The Lancet. Oncology*, 17(4), pp. 425–39. doi: 10.1016/S1470-2045(15)00613-0.

Crystal, A. S. *et al.* (2014) 'Patient-derived models of acquired resistance can identify effective drug combinations for cancer', *Science*, 346(6216), p. 1480 LP-1486. Available at: http://science.sciencemag.org/content/346/6216/1480.abstract.

Dean, J. L. *et al.* (2010) 'Therapeutic CDK4/6 inhibition in breast cancer: key mechanisms of response and failure.', *Oncogene*, 29(28), pp. 4018–32. doi: 10.1038/onc.2010.154.

Dickler, M. N. *et al.* (2016) 'MONARCH1: Results from a phase II study of abemaciclib, a CDK4 and CDK6 inhibitor, as monotherapy, in patients with HR+/HER2- breast cancer, after chemotherapy for advanced disease.', *J Clin Oncol 34*, 34.

Drake, J. M. *et al.* (2012) 'Oncogene-specific activation of tyrosine kinase networks during prostate cancer progression', *Proceedings of the National Academy of Sciences*. doi: 10.1073/pnas.1120985109.

Duncan, J. S. *et al.* (2012) 'Dynamic Reprogramming of the Kinome in Response to Targeted MEK Inhibition in Triple-Negative Breast Cancer', *Cell*, 149(2), pp. 307–321. doi: https://doi.org/10.1016/j.cell.2012.02.053.

Echalier, A. *et al.* (2014) 'An inhibitor's-eye view of the atp-binding site of CDKs in different regulatory states', *ACS Chemical Biology*, 9(6), pp. 1251–1256. doi: 10.1021/cb500135f.

Eng, J. K., McCormack, A. L. and Yates, J. R. (1994) 'An approach to correlate tandem mass spectral data of peptides with amino acid sequences in a protein database.', *Journal of the American Society for Mass Spectrometry*, 5(11), pp. 976–89. doi: 10.1016/1044-0305(94)80016-2.

Fabian, M. A. *et al.* (2005) 'A small molecule–kinase interaction map for clinical kinase inhibitors', *Nature Biotechnology*. Nature Publishing Group, 23, p. 329. Available at: http://dx.doi.org/10.1038/nbt1068.

Finn, R. S. *et al.* (2009) 'PD 0332991, a selective cyclin D kinase 4/6 inhibitor, preferentially inhibits proliferation of luminal estrogen receptor-positive human breast cancer cell lines in vitro.', *Breast cancer research : BCR*, 11(5), p. R77. doi: 10.1186/bcr2419.

Franco, J., Witkiewicz, A. K. and Knudsen, E. S. (2014) 'CDK4/6 inhibitors have potent activity in combination with pathway selective therapeutic agents in models of pancreatic cancer', *Oncotarget*, 5(15), pp. 6512–6525. doi: 10.18632/oncotarget.2270.

Fry, D. W. *et al.* (2004) 'Specific inhibition of cyclin-dependent kinase 4/6 by PD 0332991 and associated antitumor activity in human tumor xenografts', *Molecular Cancer Therapeutics*, 3(11), p. 1427 LP-1438. Available at: http://mct.aacrjournals.org/content/3/11/1427.abstract.

Gelbert, L. M. *et al.* (2014) 'Preclinical characterization of the CDK4/6 inhibitor LY2835219: in-vivo cell cycle-dependent/independent anti-tumor activities alone/in combination with gemcitabine.', *Investigational new drugs*, 32(5), pp. 825–37. doi: 10.1007/s10637-014-0120-7.

Goel, S. *et al.* (2016) 'Overcoming Therapeutic Resistance in HER2-Positive Breast Cancers with CDK4/6 Inhibitors.', *Cancer cell*, 29(3), pp. 255–69. doi: 10.1016/j.ccell.2016.02.006.

Griggs, J. J. and Wolff, A. C. (2017) 'Cyclin-Dependent Kinase 4/6 Inhibitors in the Treatment of Breast Cancer: More Breakthroughs and an Embarrassment of Riches.', *Journal of clinical oncology : official journal of the American Society of Clinical Oncology*, p. JCO2017739375. doi: 10.1200/JCO.2017.73.9375.

Hafner, M. *et al.* (2016) 'Growth rate inhibition metrics correct for confounders in measuring sensitivity to cancer drugs', *Nature Methods*, 13(6), pp. 521–527. doi: 10.1038/nmeth.3853.

Hafner, M. *et al.* (2017) 'Designing Drug-Response Experiments and Quantifying their Results', *Current Protocols in Chemical Biology*, 9.

Hafner, M., Niepel, M. and Sorger, P. K. (2017) 'Alternative drug sensitivity metrics improve preclinical cancer pharmacogenomics.', *Nature biotechnology*, 35(6), pp. 500–502. doi: 10.1038/nbt.3882.

Herrera-Abreu, M. T. *et al.* (2016) 'Early Adaptation and Acquired Resistance to CDK4/6 Inhibition in Estrogen Receptor–Positive Breast Cancer', *Cancer Research*, 76(8), pp. 2301–2313. doi: 10.1158/0008-5472.CAN-15-0728.

Horn, H. *et al.* (2014) 'KinomeXplorer: an integrated platform for kinome biology studies.', *Nature methods*, 11(6), pp. 603–4. doi: 10.1038/nmeth.2968.

Hornbeck, P. V. *et al.* (2012) 'PhosphoSitePlus: A comprehensive resource for investigating the structure and function of experimentally determined post-translational modifications in man and mouse', *Nucleic Acids Research*, 40(D1). doi: 10.1093/nar/gkr1122.

Hortobagyi, G. N. *et al.* (2016) 'Ribociclib as First-Line Therapy for HR-Positive, Advanced Breast Cancer', *New England Journal of Medicine*, 375(18), pp. 1738–1748. doi: 10.1056/NEJMoa1609709.

Kettenbach, A. N. and Gerber, S. A. (2011) 'Rapid and Reproducible Single-Stage Phosphopeptide Enrichment of Complex Peptide Mixtures: Application to General and Phosphotyrosine-Specific Phosphoproteomics Experiments', *Analytical Chemistry*, 83(20), pp. 7635–7644. doi: 10.1021/ac201894j.

Kim, S. *et al.* (2013) 'Abstract PR02: LEE011: An orally bioavailable, selective small molecule inhibitor of CDK4/6– Reactivating Rb in cancer.', *Molecular Cancer Therapeutics*, 12(11 Supplement), p. PR02 LP-PR02. Available at: http://mct.aacrjournals.org/content/12/11_Supplement/PR02.abstract.

Kitada, S. *et al.* (2000) 'Protein kinase inhibitors flavopiridol and 7-hydroxy-staurosporine down-regulate antiapoptosis proteins in B-cell chronic lymphocytic leukemia', *Blood*, 96(2), pp. 393–397. Available at: papers2://publication/uuid/D346C111-E276-4328-8AF9-4D06C2B6FB1E.

Klaeger, S. *et al.* (2017) 'The target landscape of clinical kinase drugs', *Science*, 358(6367). Available at: http://science.sciencemag.org/content/358/6367/eaan4368.abstract.

Knudsen, E. S. *et al.* (2017) 'Biological specificity of CDK4/6 inhibitors: dose response relationship, *in vivo* signaling, and composite response signature', *Oncotarget*, 8(27), pp. 43678–43691. doi: 10.18632/oncotarget.18435.

Kuleshov, M. V. *et al.* (2016) 'Enrichr: a comprehensive gene set enrichment analysis web server 2016 update', *Nucleic Acids Research*, 44(W1), pp. W90–W97. doi: 10.1093/nar/gkw377.

Lamb, J. *et al.* (2006) 'The Connectivity Map: using gene-expression signatures to connect small molecules, genes, and disease.', *Science (New York, N.Y.)*, 313(5795), pp. 1929–35. doi: 10.1126/science.1132939.

Lim, J. S. J., Turner, N. C. and Yap, T. A. (2016) 'CDK4/6 Inhibitors: Promising Opportunities beyond Breast Cancer.', *Cancer discovery*, 6(7), pp. 697–9. doi: 10.1158/2159-8290.CD-16-0563.

Lin, J.-R. *et al.* (2017) 'A simple open-source method for highly multiplexed imaging of single cells in tissues and tumours', *bioRxiv*. Available at: http://biorxiv.org/content/early/2017/06/19/151738.abstract.

Luen, S. *et al.* (2016) 'The genomic landscape of breast cancer and its interaction with host immunity', *Breast*, 29, pp. 241–250. doi: 10.1016/j.breast.2016.07.015.

McAlister, G. C. *et al.* (2012) 'Increasing the multiplexing capacity of TMTs using reporter ion

isotopologues with isobaric masses.', *Analytical chemistry*, 84(17), pp. 7469–78. doi: 10.1021/ac301572t.

McAlister, G. C. *et al.* (2014) 'MultiNotch MS3 enables accurate, sensitive, and multiplexed detection of differential expression across cancer cell line proteomes.', *Analytical chemistry*, 86(14), pp. 7150–8. doi: 10.1021/ac502040v.

McCain, J. (2015) 'First-in-Class CDK4/6 Inhibitor Palbociclib Could Usher in a New Wave of Combination Therapies for HR+, HER2- Breast Cancer.', *P & T : a peer-reviewed journal for formulary management*, 40(8), pp. 511–20. Available at: http://www.pubmedcentral.nih.gov/articlerender.fcgi?artid=4517534&tool=pmcentrez&rendertype=abstract.

McCarthy, D. J., Chen, Y. and Smyth, G. K. (2012) 'Differential expression analysis of multifactor RNA-Seq experiments with respect to biological variation', *Nucleic Acids Research*, 40(10), pp. 4288–4297. Available at: http://dx.doi.org/10.1093/nar/gks042.

Médard, G. *et al.* (2015) 'Optimized Chemical Proteomics Assay for Kinase Inhibitor Profiling', *Journal of Proteome Research*. American Chemical Society, 14(3), pp. 1574–1586. doi: 10.1021/pr5012608.

Meloche, S. and Pouysségur, J. (2007) 'The ERK1/2 mitogen-activated protein kinase pathway as a master regulator of the G1- to S-phase transition', *Oncogene*, 26(22), pp. 3227–3239. doi: 10.1038/sj.onc.1210414.

O'Brien, N. *et al.* (2018) 'Preclinical Activity of Abemaciclib Alone or in Combination with Antimitotic and Targeted Therapies in Breast Cancer', *Molecular Cancer Therapeutics*, 17(5), p. 897 LP-907. Available at: http://mct.aacrjournals.org/content/17/5/897.abstract.

O'Leary, B., Finn, R. S. and Turner, N. C. (2016) 'Treating cancer with selective CDK4/6 inhibitors', *Nature Reviews Clinical Oncology*. Nature Publishing Group, 13(7), pp. 417–430. doi: 10.1038/nrclinonc.2016.26.

O'Brien, N. A. *et al.* (2014) 'Abstract 4756: In vivo efficacy of combined targeting of CDK4/6, ER and PI3K signaling in ER+ breast cancer', *Cancer Research*, 74(19 Supplement), p. 4756 LP-4756. Available at: http://cancerres.aacrjournals.org/content/74/19_Supplement/4756.abstract.

Palechor-Ceron, N. *et al.* (2013) 'Radiation Induces Diffusible Feeder Cell Factor(s) That Cooperate with ROCK Inhibitor to Conditionally Reprogram and Immortalize Epithelial Cells', *The American Journal of Pathology*, 183(6), pp. 1862–1870. doi: 10.1016/j.ajpath.2013.08.009.

Patnaik, A., Rosen, L. S., *et al.* (2016) 'Efficacy and Safety of Abemaciclib, an Inhibitor of CDK4 and CDK6, for Patients with Breast Cancer, Non–Small Cell Lung Cancer, and Other Solid Tumors', *Cancer Discovery*, 6(7). Available at: http://cancerdiscovery.aacrjournals.org/content/6/7/740 (Accessed: 2 May 2017).

Patnaik, A., Rosen, L. S., *et al.* (2016) 'Single-Agent Abemaciclib Active in Breast Cancer.', *Cancer discovery*, 6(8), pp. 809–10. doi: 10.1158/2159-8290.CD-NB2016-081.

Paulo, J. A. *et al.* (2015) 'Effects of MEK inhibitors GSK1120212 and PD0325901 in vivo using 10-plex quantitative proteomics and phosphoproteomics.', *Proteomics*, 15(2–3), pp. 462–73. doi:

10.1002/pmic.201400154.

Peplow, M. (2017) 'Astex shapes CDK4/6 inhibitor for approval', *Nature biotechnology*, 35, pp. 395–396.

Rappsilber, J., Mann, M. and Ishihama, Y. (2007) 'Protocol for micro-purification, enrichment, pre-fractionation and storage of peptides for proteomics using StageTips.', *Nature protocols*, 2(8), pp. 1896–906. doi: 10.1038/nprot.2007.261.

Raub, T. J. *et al.* (2015) 'Brain Exposure of Two Selective Dual CDK4 and CDK6 Inhibitors and the Antitumor Activity of CDK4 and CDK6 Inhibition in Combination with Temozolomide in an Intracranial Glioblastoma Xenograft', *Drug Metabolism and Disposition*, 43(9), p. 1360 LP-1371. Available at: http://dmd.aspetjournals.org/content/43/9/1360.abstract.

Reid, Y. *et al.* (2004) *Authentication of Human Cell Lines by STR DNA Profiling Analysis*, *Assay Guidance Manual*. Available at: http://www.ncbi.nlm.nih.gov/pubmed/23805434.

Riley, N. M. and Coon, J. J. (2016) 'Phosphoproteomics in the Age of Rapid and Deep Proteome Profiling', *Analytical Chemistry*, 88(1), pp. 74–94. doi: 10.1021/acs.analchem.5b04123.

Robinson, M. D., McCarthy, D. J. and Smyth, G. K. (2010) 'edgeR: a Bioconductor package for differential expression analysis of digital gene expression data', *Bioinformatics*, 26(1), pp. 139–140. doi: 10.1093/bioinformatics/btp616.

Schwanhäusser, B. *et al.* (2011) 'Global quantification of mammalian gene expression control', *Nature*. Nature Publishing Group, a division of Macmillan Publishers Limited. All Rights Reserved., 473, p. 337. Available at: https://doi.org/10.1038/nature10098.

Sherr, C. J., Beach, D. and Shapiro, G. I. (2016) 'Targeting CDK4 and CDK6: From Discovery to Therapy.', *Cancer discovery*, 6(4), pp. 353–67. doi: 10.1158/2159-8290.CD-15-0894.

Sledge, G. W. *et al.* (2017) 'MONARCH 2: Abemaciclib in Combination With Fulvestrant in Women With HR+/HER2- Advanced Breast Cancer Who Had Progressed While Receiving Endocrine Therapy.', *Journal of clinical oncology : official journal of the American Society of Clinical Oncology*, p. JCO2017737585. doi: 10.1200/JCO.2017.73.7585.

Soumillon, M. *et al.* (2014) 'Characterization of directed differentiation by high-throughput single-cell RNA-Seq', *bioRxiv*. Available at: http://biorxiv.org/content/early/2014/03/05/003236.abstract.

Srivastava, A. *et al.* (2016) 'RapMap: a rapid, sensitive and accurate tool for mapping RNA-seq reads to transcriptomes.', *Bioinformatics (Oxford, England)*. England, 32(12), pp. i192–i200. doi: 10.1093/bioinformatics/btw277.

Subramanian, A. *et al.* (2005) 'Gene set enrichment analysis: A knowledge-based approach for interpreting genome-wide expression profiles', *Proceedings of the National Academy of Sciences*, 102(43), pp. 15545–15550. doi: 10.1073/pnas.0506580102.

Svensson, V. *et al.* (2017) 'Power analysis of single-cell RNA-sequencing experiments', *Nature Methods*. Nature Publishing Group, a division of Macmillan Publishers Limited. All Rights Reserved., 14, p. 381. Available at: http://dx.doi.org/10.1038/nmeth.4220.

Ting, L. *et al.* (2011) 'MS3 eliminates ratio distortion in isobaric multiplexed quantitative proteomics.', *Nature methods*, 8(11), pp. 937–40. doi: 10.1038/nmeth.1714.

Toogood, P. L. *et al.* (2005) 'Discovery of a potent and selective inhibitor of cyclin-dependent kinase 4/6', *Journal of Medicinal Chemistry*, 48(7), pp. 2388–2406. doi: 10.1021/jm049354h.

Torres-guzmán, R. *et al.* (2017) 'Preclinical characterization of abemaciclib in hormone receptor positive breast cancer'.

Wittmann, S. *et al.* (2003) 'Flavopiridol down-regulates antiapoptotic proteins and sensitizes human breast cancer cells to epothilone B-induced apoptosis', *Cancer Research*, 63(1), pp. 93–99.

Yang, C. *et al.* (2017) 'Acquired CDK6 amplification promotes breast cancer resistance to CDK4/6 inhibitors and loss of ER signaling and dependence', *Oncogene*, 36(16), pp. 2255–2264. doi: 10.1038/onc.2016.379.

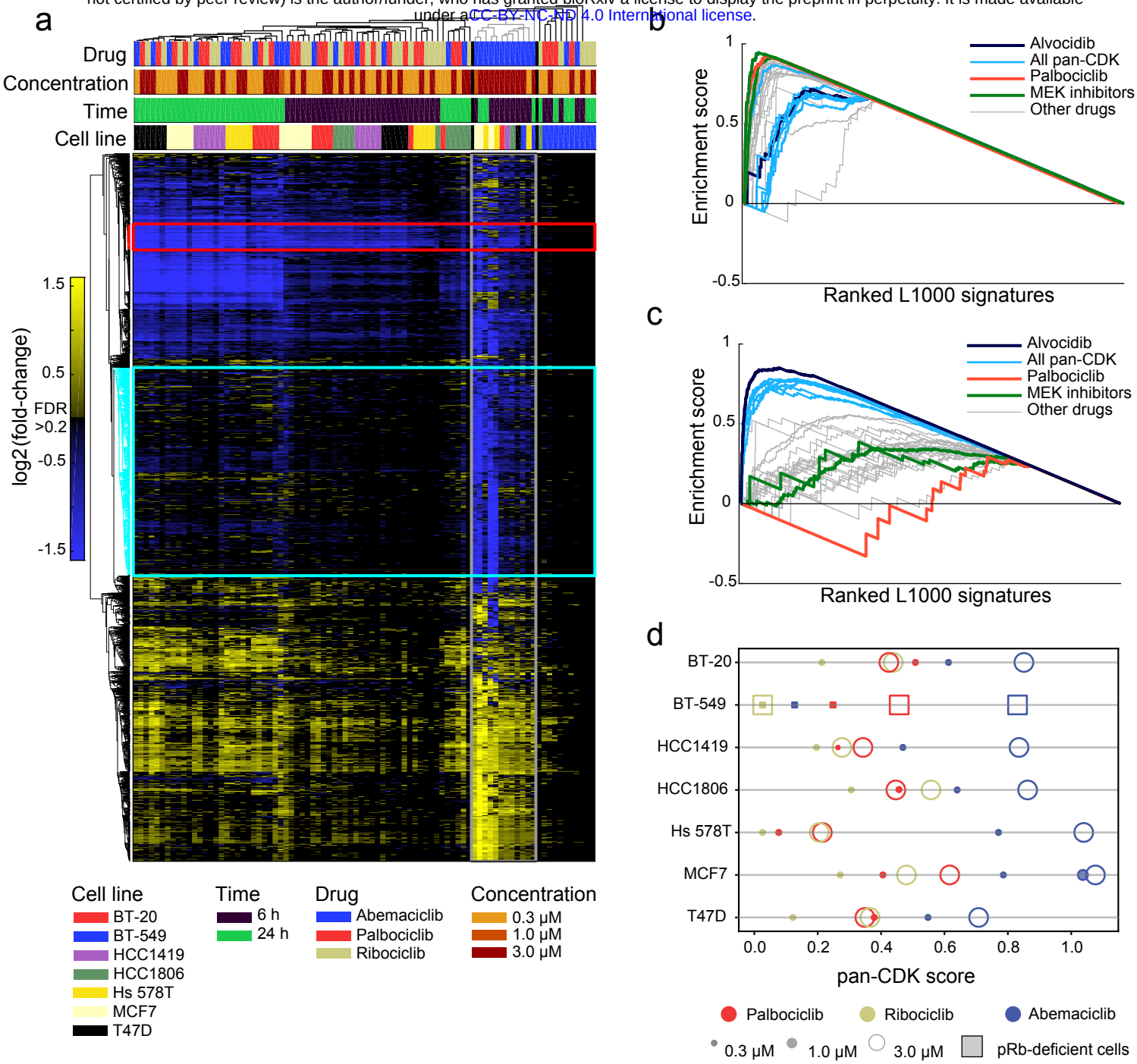

Figure 1

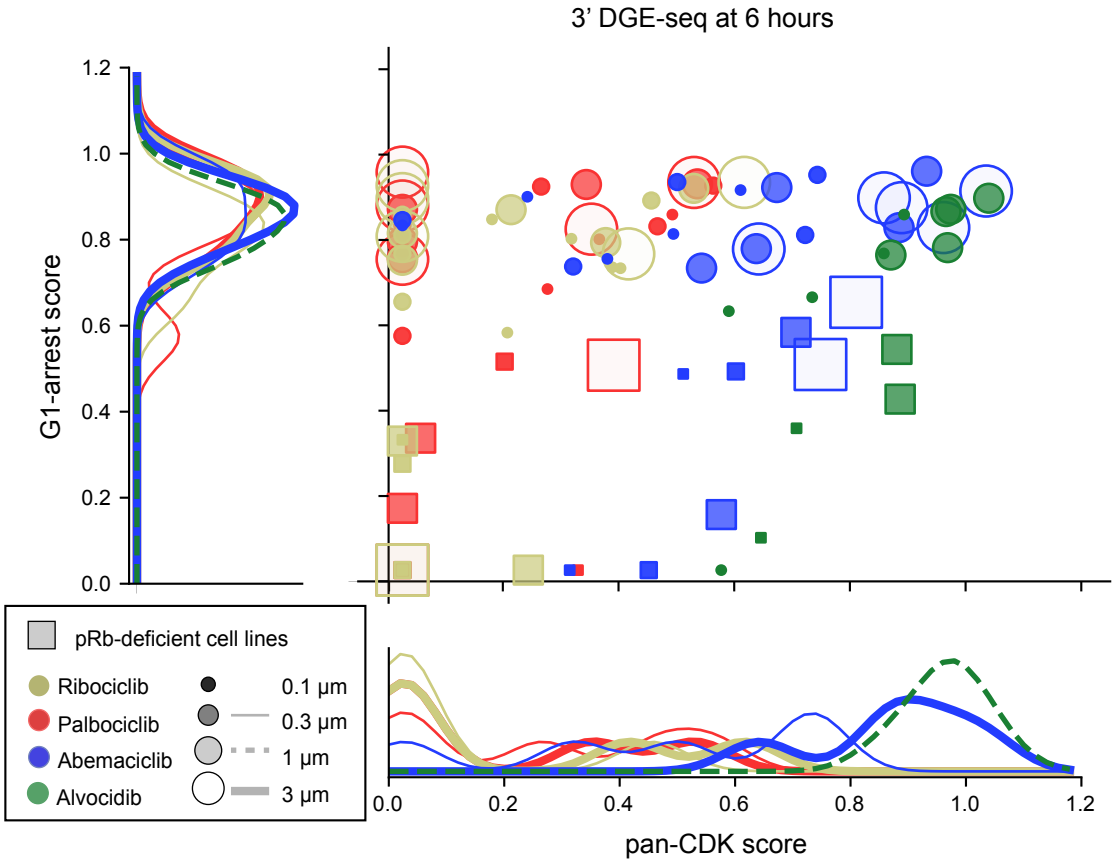

Figure 2

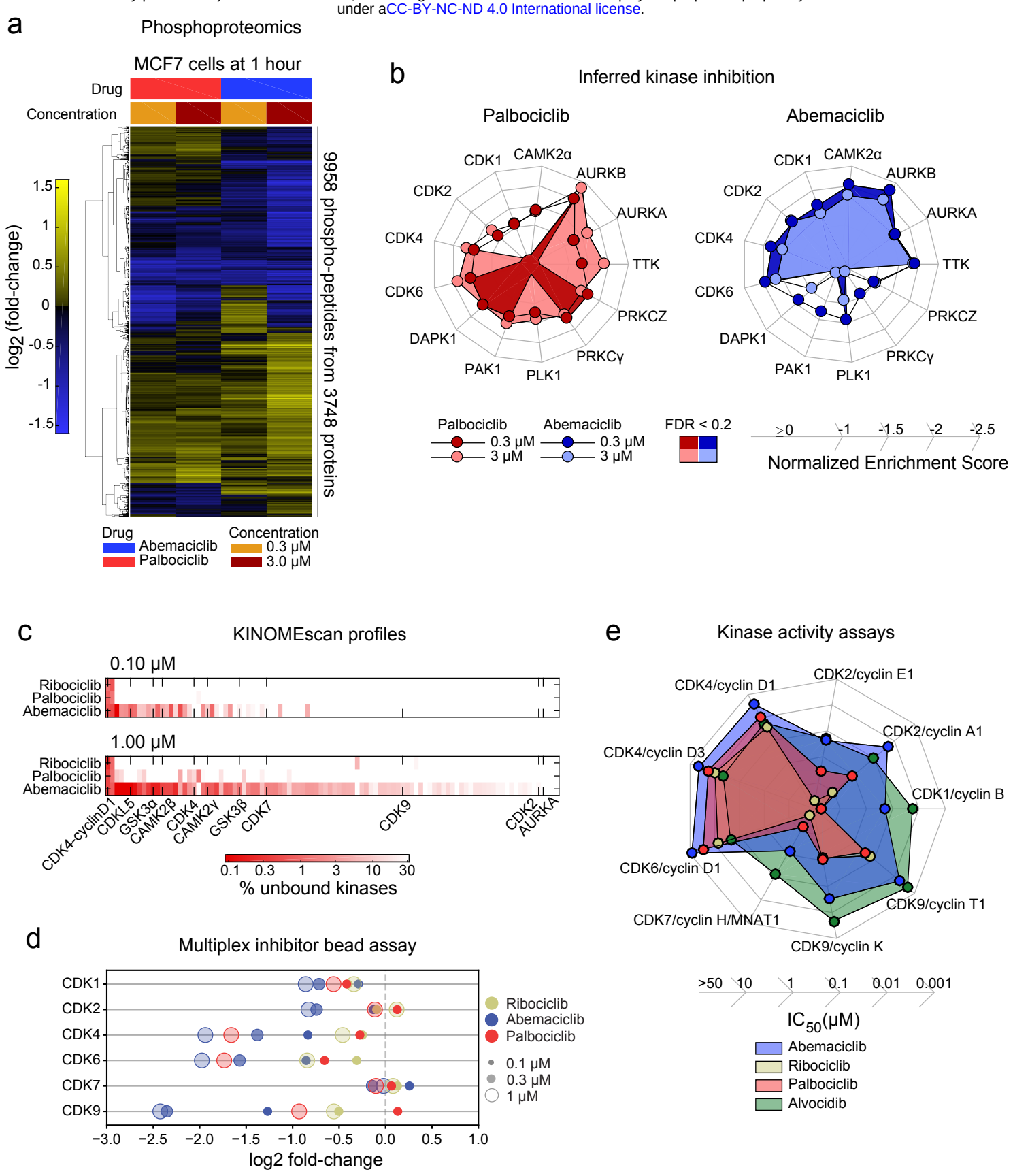

Figure 3

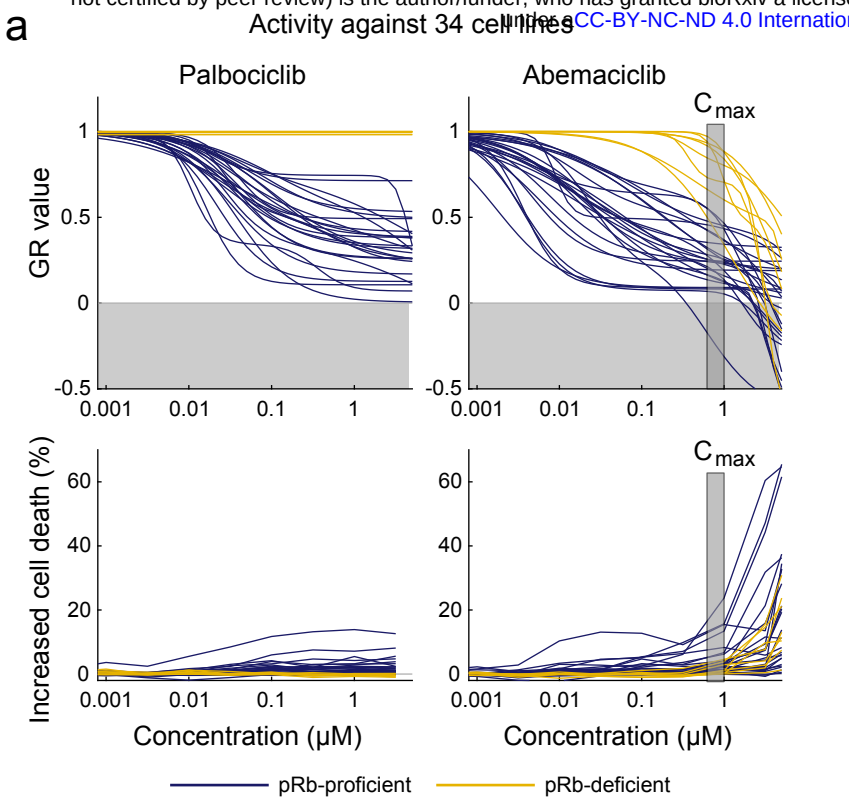

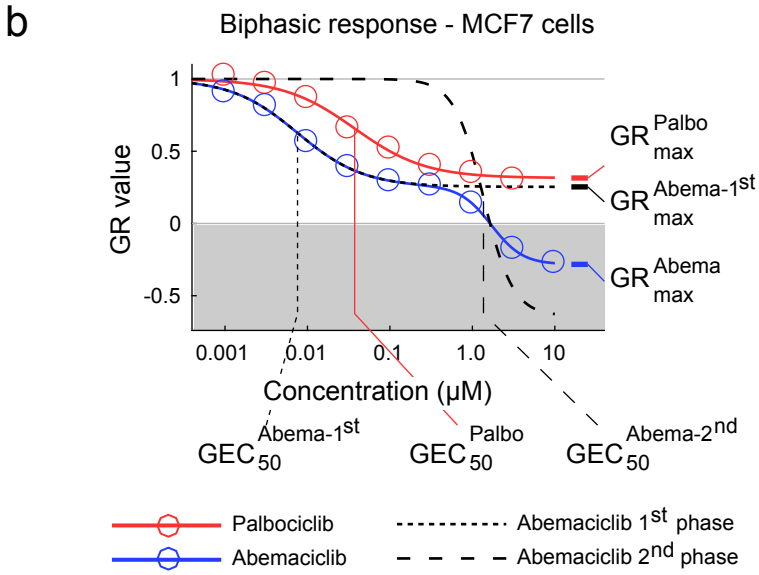

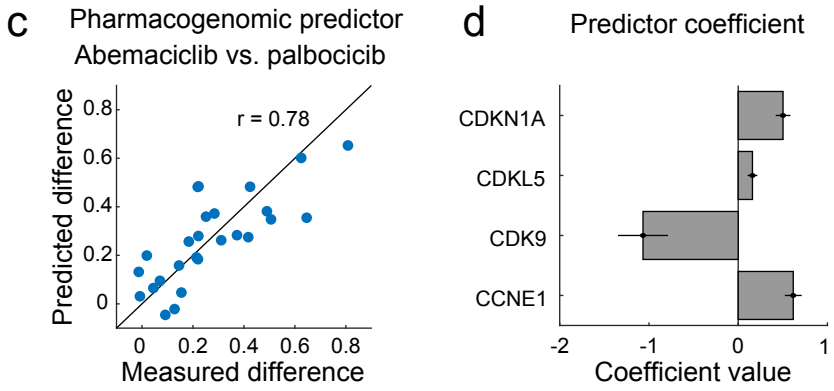

Figure 4

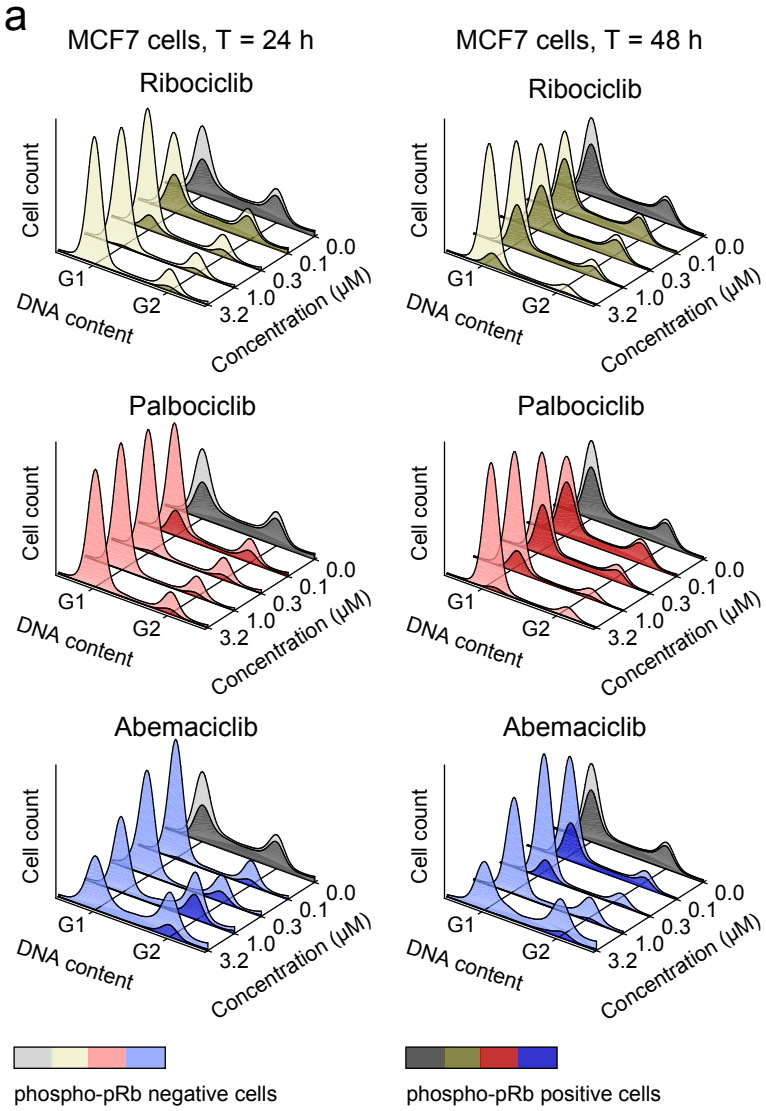

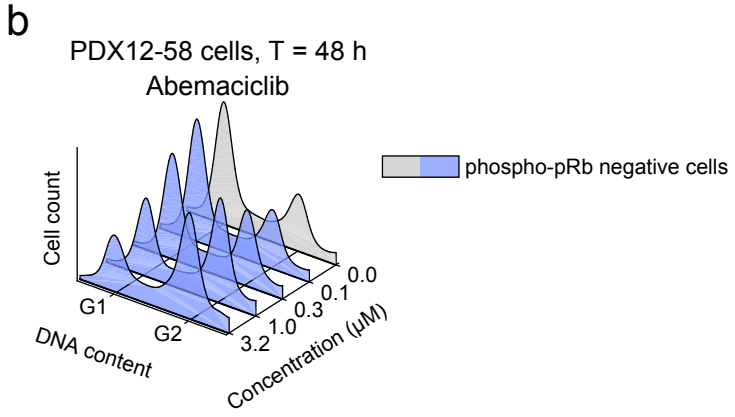

Figure 5

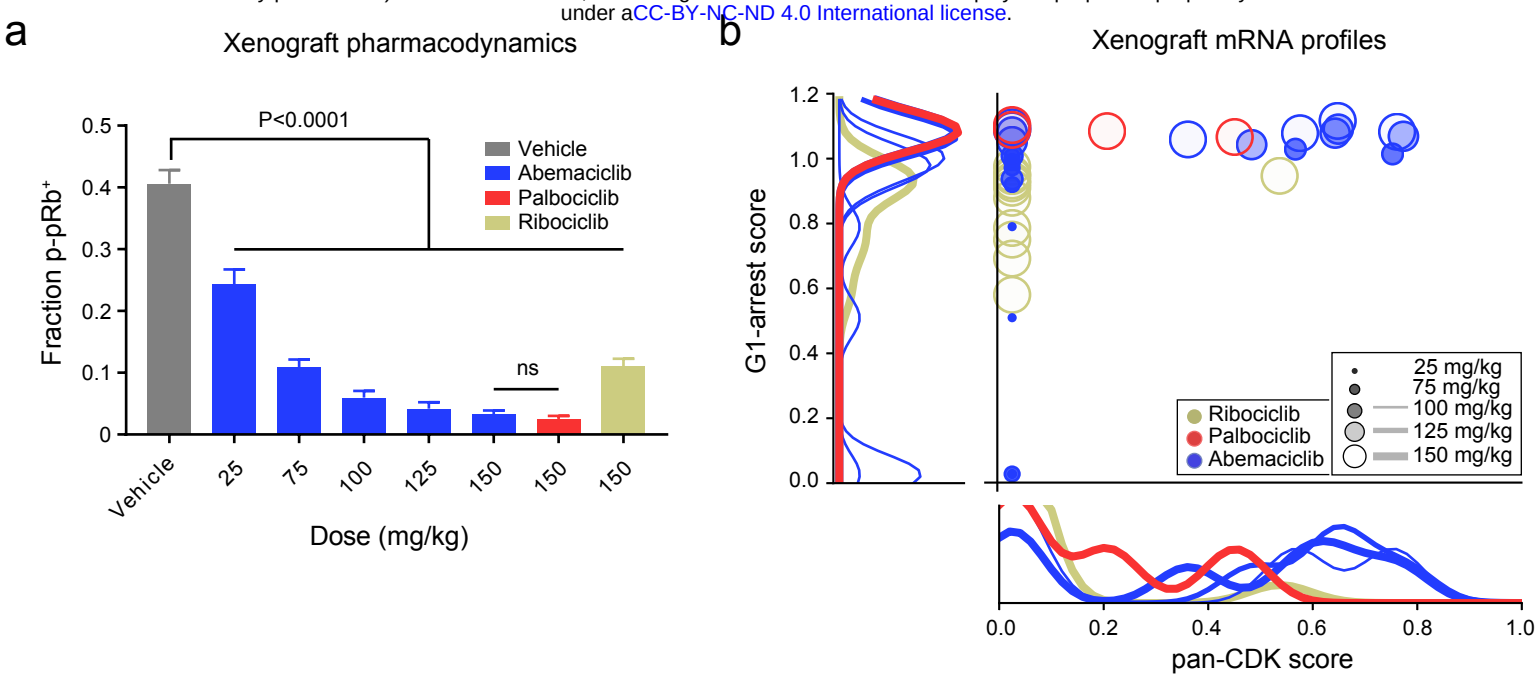

Figure 6

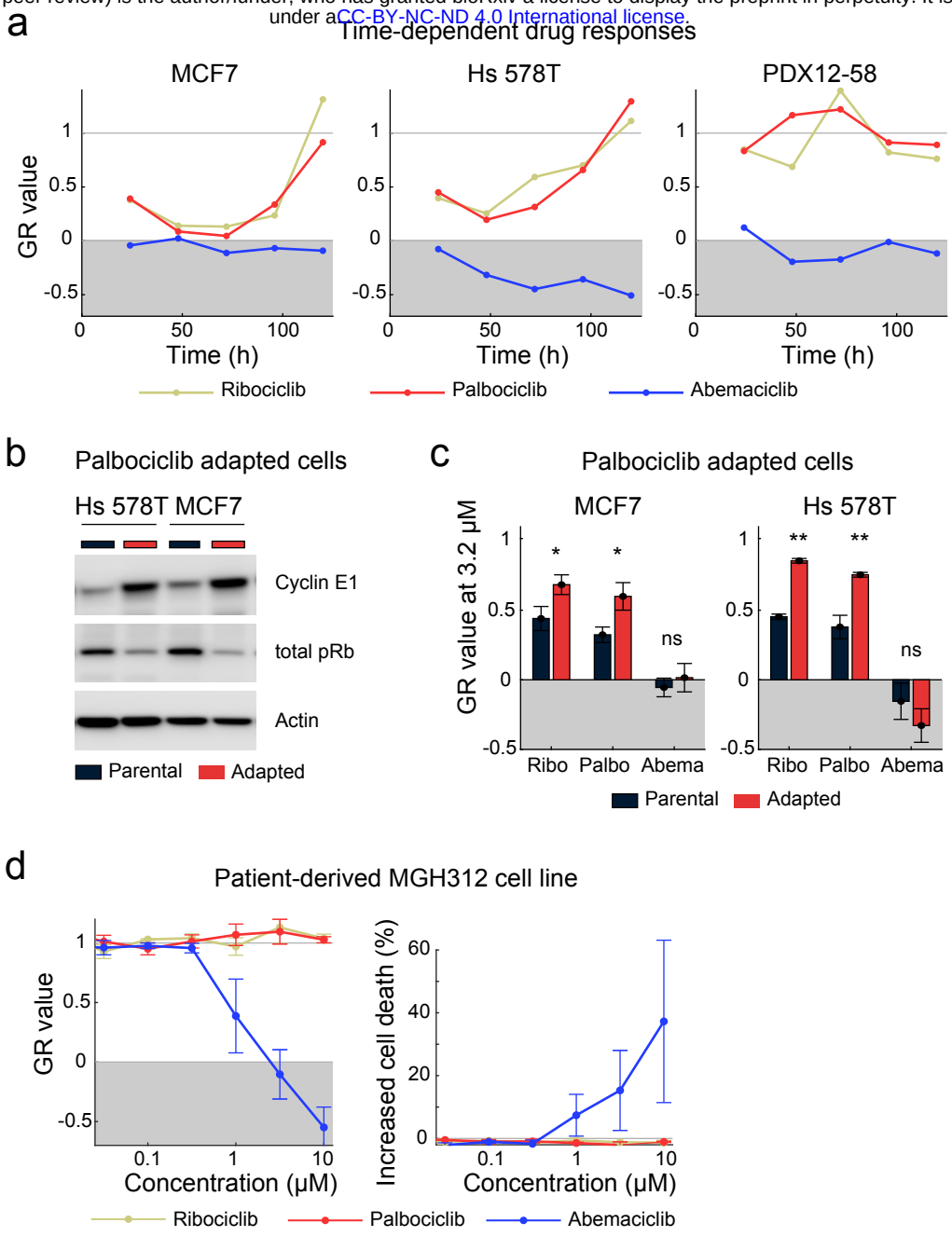

Figure 7

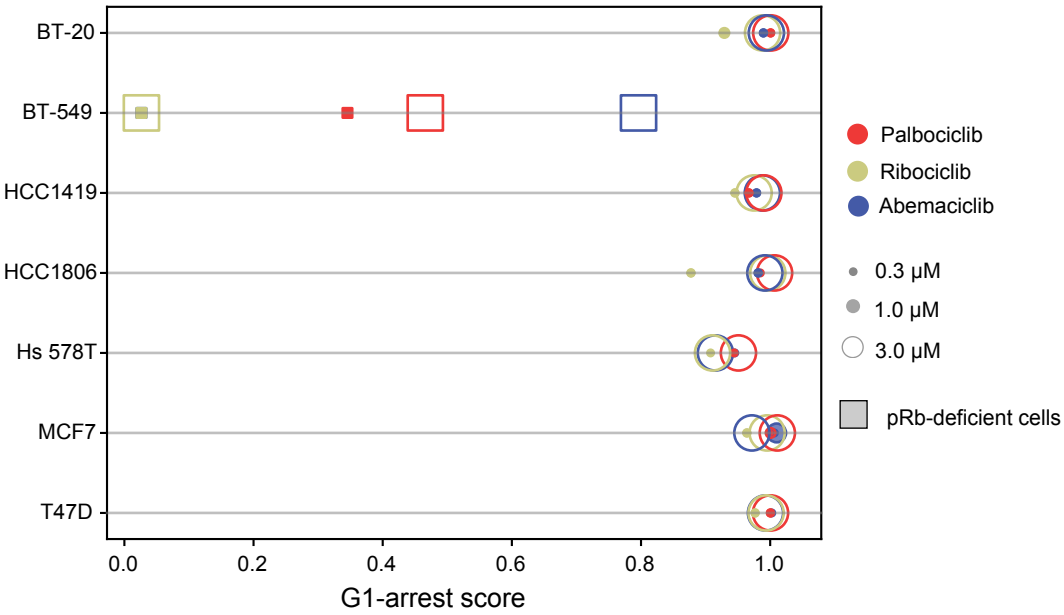

Figure S1. Related to Figure 1.

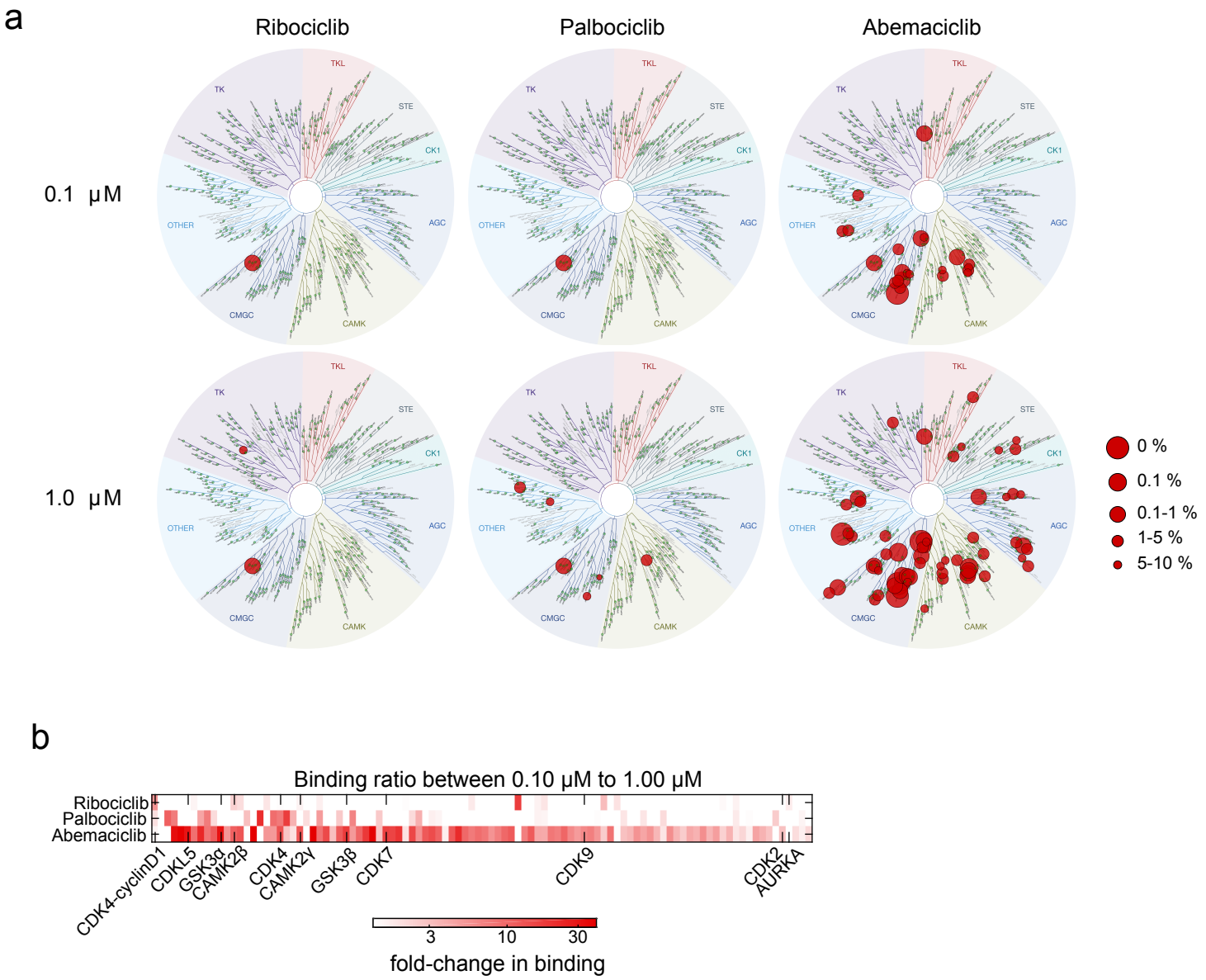

Figure S2. Related to Figure 3.

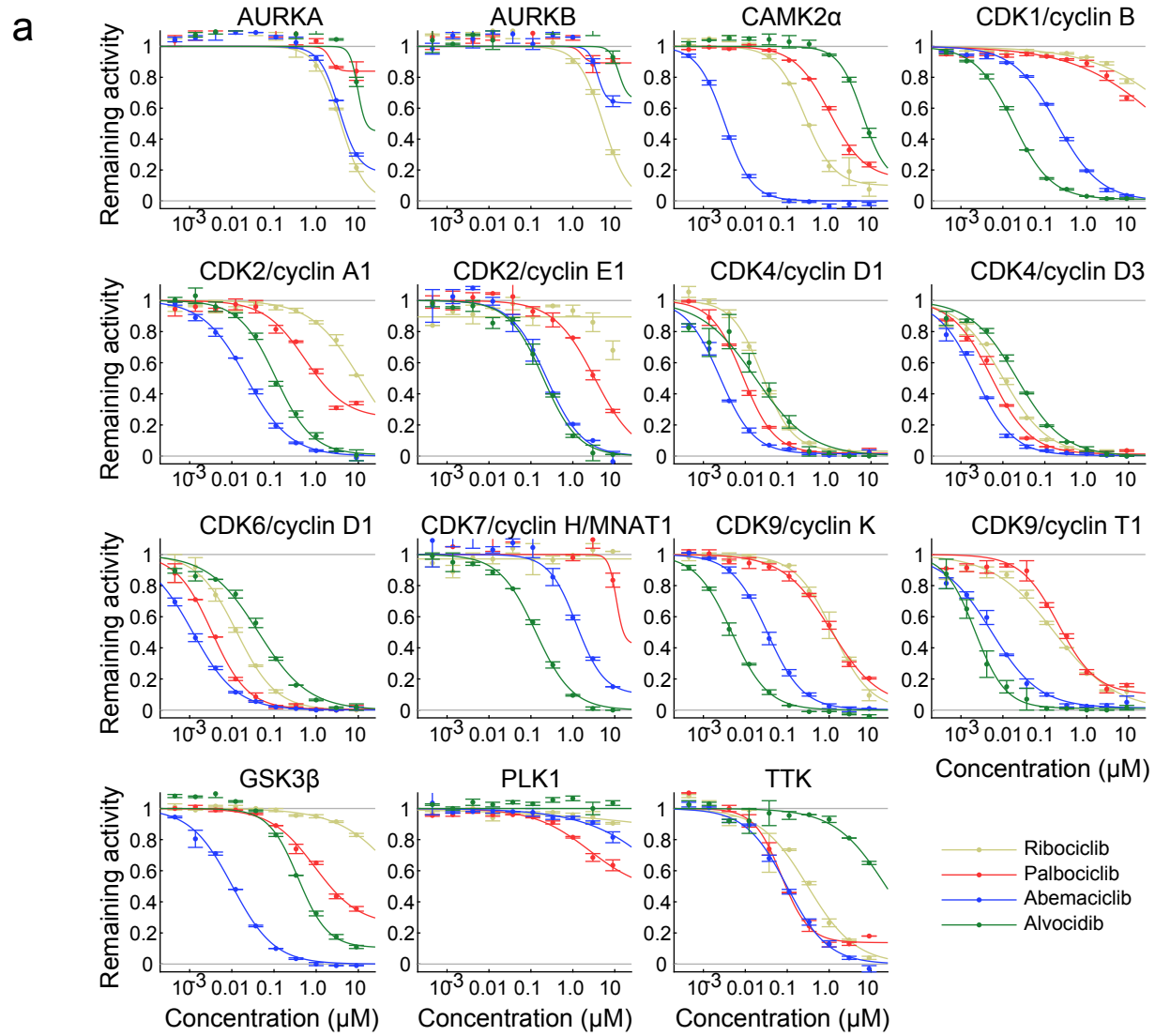

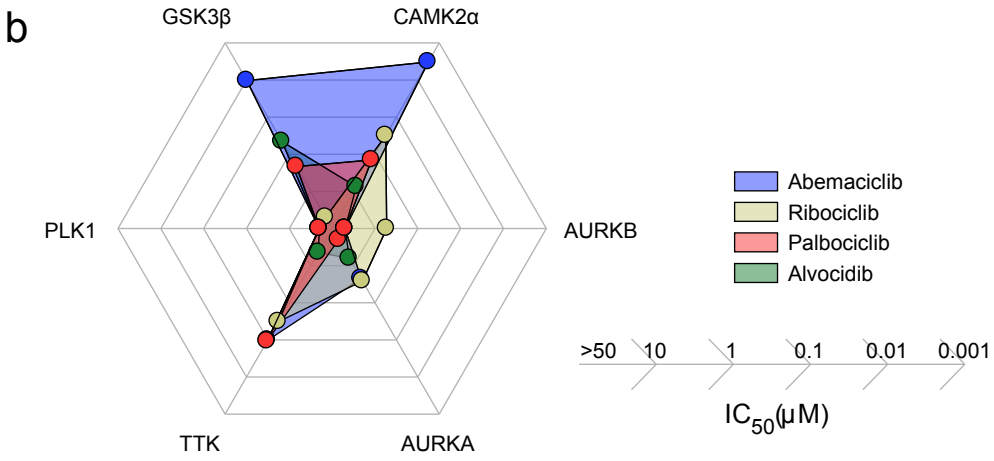

Figure S3. Related to Figure 3.

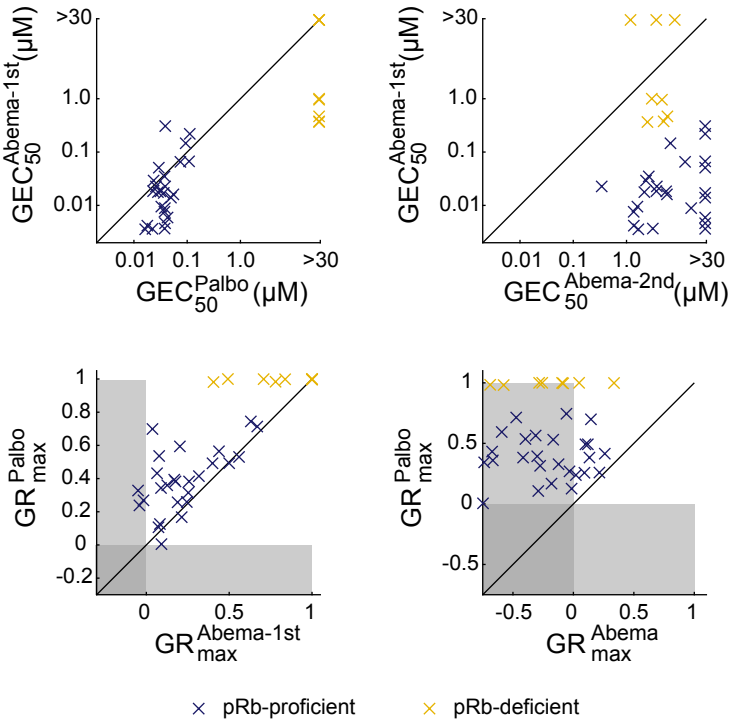

Figure S4. Related to Figure 4.

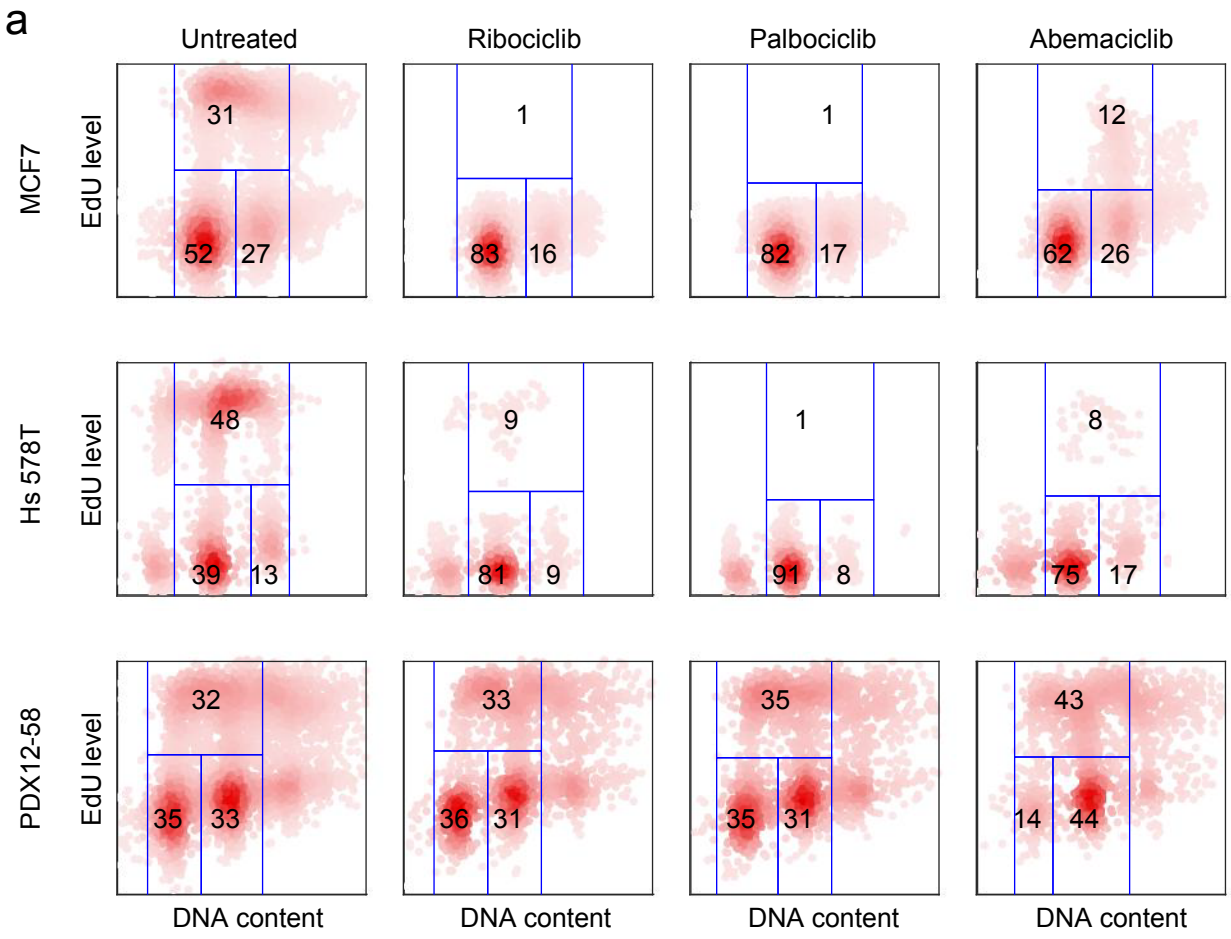

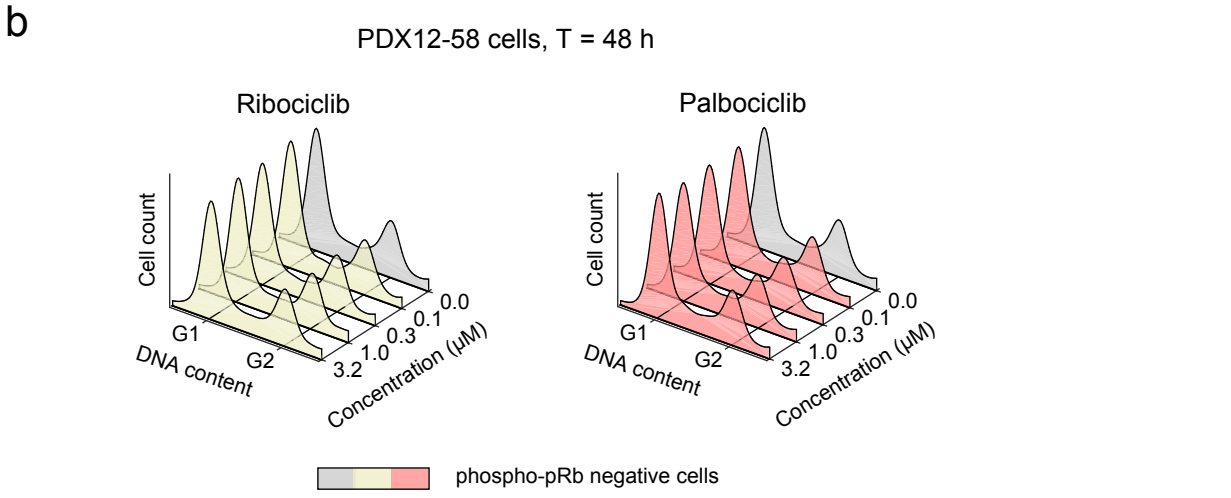

Figure S5. Related to Figure 5.

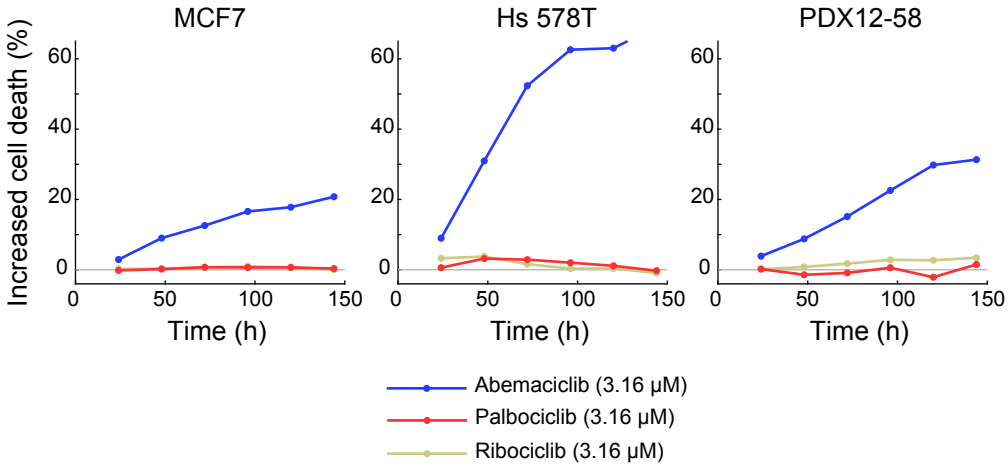

Figure S6. Related to Figure 7.

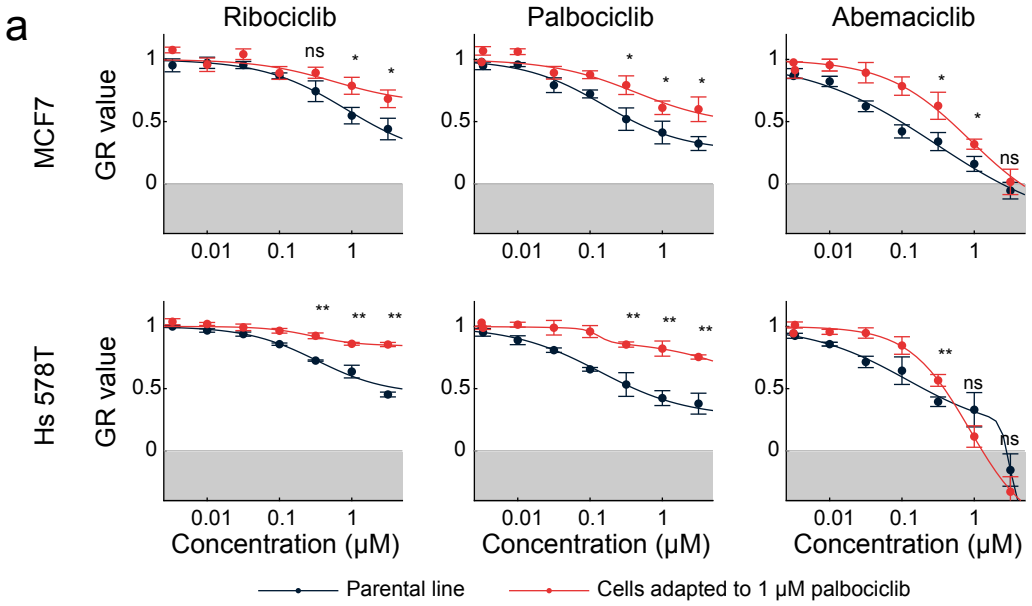

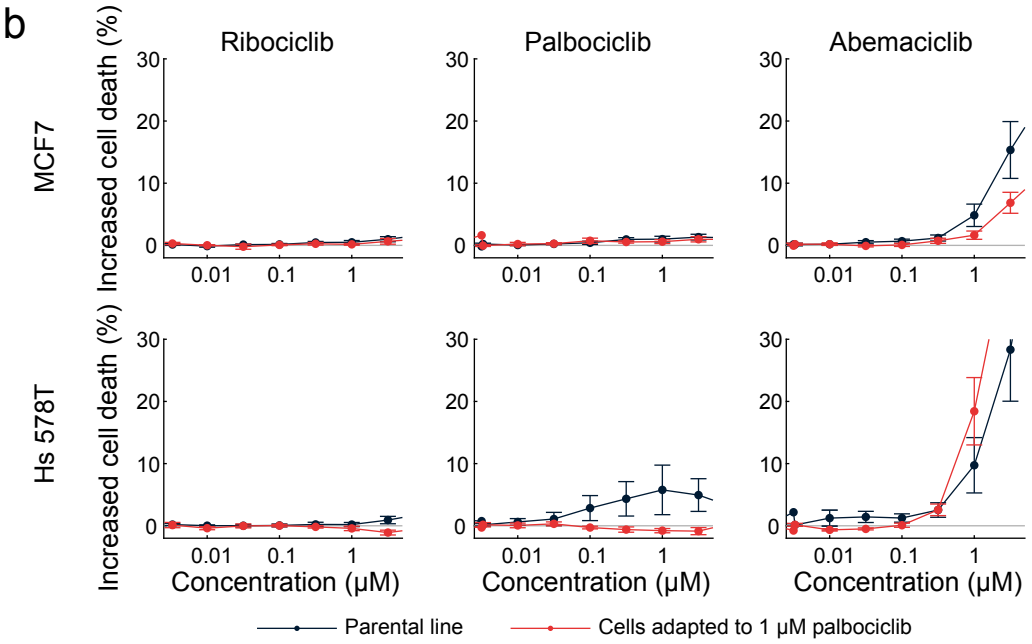

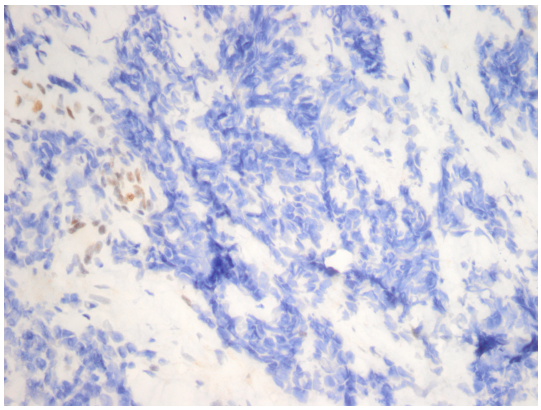

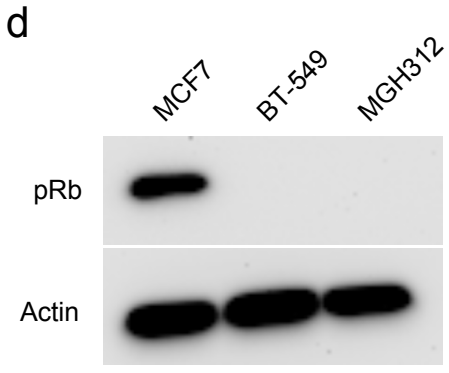

Figure S7. Related to Figure 7.